Geobiology (2005), **3**, 53–76

A coupled atmosphere–ecosystem model of the early Archean Earth

P. KHARECHA,[1,3] J. KASTING[1] AND J. SIEFERT[2]

[1] *Department of Geosciences and Astrobiology Research Center, Pennsylvania State University, University Park, PA 16802, USA*
[2] *Department of Statistics, Rice University, Houston, TX 77251, USA*
[3] *NASA Goddard Institute for Space Studies (Columbia University), New York, NY 10025, USA*

ABSTRACT

A coupled photochemical-ecosystem model has been developed to simulate the early Archean biosphere. The model incorporates kinetic and nutrient limitations on biological productivity, along with constraints imposed by metabolic thermodynamics. We have used this model to predict the biogenic CH_4 flux and net primary productivity (NPP) of the marine biosphere prior to the advent of oxygenic photosynthesis. Organisms considered include chemotrophic and organotrophic methanogens, H_2-, H_2S-, and Fe-using anoxygenic phototrophs, S-reducing bacteria, CO-using acetogens, and fermentative bacteria.

CH_4 production and NPP in our model are limited by the downward flux of H_2, CO, S_8, and H_2S through the atmosphere–ocean interface and by the upwelling rate of Fe^{2+} from the deep oceans. For reasonable estimates of the supply rates of these compounds, we find that the biogenic CH_4 flux should have ranged from approximately $^1/_3$ to 2.5 times the modern CH_4 flux. In the anoxic Archean atmosphere, this would have produced CH_4 concentrations of 100 ppmv to as much as 35 000 ppmv (3.5%), depending on the rate at which hydrogen escaped to space. Recent calculations indicating that hydrogen escape was slow favour the higher CH_4 concentrations. Calculated NPP is lower than in the modern oceans by a factor of at least 40. In our model, H_2-based metabolism is moderately more productive than Fe^{2+}-based metabolism, with S-based metabolism being considerably less productive. Internal recycling of sulphur within the surface ocean could conceivably raise rates of sulphur metabolism by a factor of 10 higher than the values predicted by our model.

Although explicit climate calculations have not been performed here, our results are consistent with the idea that the Archean climate was warm, and possibly very hot. Some or most of our ecosystem scenarios are consistent with the carbon isotope record, depending on how that record is interpreted. If the conventional view is correct and organic carbon burial accounted for approximately 20% of total carbon burial during the Archean, then only two of our phototroph-based model ecosystems are plausible. However, if a recent alternative analysis is correct and only approximately 0–10% of total buried carbon was organic, then essentially all of our anaerobic ecosystems are plausible. A better understanding of both the geochemical and the biological records is needed to better constrain our models.

Received 26 May 2005; accepted 8 September 2005

Corresponding author: P. Kharecha. Tel.: 814-863-7689; fax: 814-863-2001; e-mail: pushker@essc.psu.edu.

INTRODUCTION

Previous studies by our group (Kasting *et al.*, 1983; Pavlov *et al.*, 2000, 2001a,b) and by others (Zahnle, 1986; Kiehl & Dickinson, 1987; Catling *et al.*, 2001) have explored the photochemistry of methane in an anoxic early Earth atmosphere and have examined its effect on climate and on redox evolution of the crust. Two other studies (Kral *et al.*, 1998; Kasting *et al.*, 2001) have looked at the coupling between the Archean atmosphere and a hypothetical methanogenic ecosystem, but only in a pure thermodynamic sense and only in isolation from other likely components of an anaerobic Archean biosphere. Another recent study assessed the productivity of S- and Fe^{2+}-based Archean ecosystems but did not explicitly consider H_2-based metabolism (Canfield, 2005). Here, we present a more detailed analysis of the Archean ecosystem in which we estimate the relative productivity of H_2-, S-, and Fe^{2+}-based metabolism based on both kinetic and thermodynamic constraints. We are interested specifically in methane because of its importance to climate, along with its

possible significance as a biomarker on extrasolar planets. However, we hope that our model will also elucidate the relative importance of different metabolisms, and in doing so, shed light on the general pattern of biological/ecological evolution during the early stages of Earth history.

According to standard solar evolution models (e.g. Gough, 1981), the Sun was considerably dimmer in the past – a change that is best countered by an increased greenhouse effect in Earth's atmosphere. Besides CO_2 and H_2O, the favoured greenhouse gas is CH_4 (Kiehl & Dickinson, 1987; Pavlov *et al.*, 2000). On the present Earth, biotic sources for CH_4 outweigh abiotic ones. The ratio of biotic to abiotic CH_4 was estimated to be approximately 300 (Kasting & Catling, 2003), based on an extrapolation of measurements of dissolved CH_4 in hydrothermal vent fluids emanating from the Lost City vent field (Kelley *et al.*, 2001). New measurements (Kelley *et al.*, 2005) indicate that dissolved CH_4 concentrations at Lost City are higher than first thought by about a factor of 10; hence, the ratio of biotic to abiotic CH_4 may only be approximately 30. Biotic production of CH_4 probably outweighed abiotic production in the early Archean as well. Here, we estimate the global biotic production rate of CH_4 during the early- to mid-Archean (approximately 3.8–3.0 Ga), *before* the advent of oxygenic photosynthesis. We consider the identification of cyanobacterial and eukaryotic organic biomarkers in 2.7-Ga sediments by Brocks *et al.* (1999) as the earliest convincing evidence for oxygenic photosynthesis. After the origin of oxygenic photosynthesis, CH_4 production rates may have increased substantially as a consequence of increased production of organic matter (Catling *et al.*, 2001). This only strengthens the conclusion reached here that methane was abundant enough to exert a major effect on Archean atmospheric chemistry and climate.

The primary goal of this study is therefore to estimate the concentration of biogenic CH_4 in the Archean atmosphere. A secondary goal is to assess the supply of nutrients to the global biota and to estimate global primary productivity. In the modern biosphere, primary productivity is limited mainly by the availability of fixed nitrogen (N), phosphate (P), and iron (e.g. Tyrrell, 1999). However, before the advent of oxygenic photosynthesis, the main limitation on productivity was probably the availability of electron donors such as H_2, CO, H_2S, and dissolved Fe^{2+} (Walker, 1977; DesMarais, 1998). In the anoxic Archean atmosphere, the three reduced gases would have had long atmospheric lifetimes and could have accumulated to substantial levels (Walker, 1977; Pavlov *et al.*, 2001a,b). Their transfer rates to the surface ocean, or to soils, would have been limited by diffusion and can thus be estimated quantitatively. Ferrous iron (Fe^{2+}) was abundant in the deep ocean and would have been supplied to the surface biosphere by upwelling at rates that can also be estimated quantitatively (Holland, 1984). These kinetic constraints are modelled explicitly in the present study, and the results are compared with those found using alternative approaches (Canfield, 2005).

Determining the concentrations of biogenic gases in the Archean atmosphere could provide useful information for the search for extraterrestrial life. Within the next 10–15 years, NASA's two planned Terrestrial Planet Finder (TPF) missions will attempt to detect possible biosignatures in the atmospheres of Earth-like extrasolar planets. Methane is one of the potential biosignature gases in such atmospheres (Schindler & Kasting, 2000). An issue that is relevant for TPF is how much methane should be present on an inhabited planet compared to an uninhabited one. The present study helps shed light on this question.

We begin by outlining some general characteristics of the early Archean biosphere and discussing the types of primary producers that likely existed during that period.

NATURE OF THE ARCHEAN BIOSPHERE

As a starting point, we assume that both net primary productivity (NPP) and methane production during the Archean were dominated by ecosystems that were primarily marine rather than terrestrial. Today, of course, this is not the case. Rates of terrestrial and marine NPP are roughly equivalent: approximately 60 Gt C $year^{-1}$ for land plants and approximately 45 Gt C $year^{-1}$ for marine ecosystems (Prentice *et al.*, 2001). Modern terrestrial productivity, however, is dominated by vascular plants, which did not evolve until the Late Silurian period, approximately 440 Ma. By contrast, Archean organisms were strictly unicellular, or at most filamentous forms of bacteria. Microbial life was evidently present in Archean soils, as inferred from isotopically light organic carbon recovered from 2.6-billion-year-old palaeosols (Watanabe *et al.*, 2000). However, in the absence of vascular plants and their extended root systems, the extent of microbial colonization of the land surface was probably small. The difficulty in colonizing the land surface may have been exacerbated by the high solar UV fluxes expected prior to the development of an effective ozone shield (Ratner & Walker, 1972; Pavlov *et al.*, 2001a). We therefore neglect terrestrial life, recognizing that any such life that was present would only add to the productivity figures estimated here.

Similar considerations apply to methanogenic ecosystems and biological methane production. Today, most biogenic methane originates from terrestrial environments such as wetlands, rice paddies, and cattle farms. Substantial amounts of methane are also produced at depth in marine sediments; however, little of it escapes to the overlying ocean and atmosphere. Instead, it is consumed by aerobic methanotrophs and by consortia of anaerobic methanotrophs and sulphate reducers that use dissolved O_2 and sulphate, respectively, to oxidize the methane (Hayes, 1983; Hinrichs *et al.*, 1999). By contrast, during the Archean the deep ocean was devoid of O_2 and low in sulphate (Canfield, 1998; Canfield *et al.*, 2000; Huston & Logan, 2004). Thus, both the oceans and the marine sediments should have afforded ideal habitats for anaerobic

micro-organisms such as methanogens. We therefore feel justified in focusing our attention there, recognizing once again that production of methane by terrestrial ecosystems would only add to the numbers estimated here.

Limitations on primary productivity in the modern and Archean marine biospheres

In the modern marine biosphere, primary production is dominated by oxygenic photosynthesis ($CO_2 + H_2O + h\nu \rightarrow CH_2O + O_2$), and the global NPP is approximately 45 Gt C year^{-1} or approximately 3.8×10^{15} mol C year^{-1} (Prentice *et al.*, 2001). Except at very high latitudes where the photon flux is small, marine productivity is limited by the availability of three nutrients: N (as nitrate), P (as phosphate), and in some locations, Fe. Tyrrell (1999) has developed a model of the modern marine biosphere in which P is the ultimate limiting nutrient (i.e. limiting on long time scales) and N is the proximate limiting nutrient (limiting on relatively short time scales). In his model, biological nitrogen fixation keeps pace with P availability, so that it is P, not N, that ultimately determines primary productivity. He assumes a flux balance in which P is supplied to the oceans by riverine input (ultimately by weathering of rocks on the continents) at a global rate of approximately 10^{11} mol year^{-1}, and is removed as a constituent of organic matter. In reality, P is also removed from the oceans by adsorption onto iron oxyhydroxides precipitating in hydrothermal plumes, and as a component of evaporite deposits (Van Cappellen & Ingall, 1996).

In the anaerobic Archean marine biosphere, once biological nitrogen fixation had been invented, N should not have been an ultimate limiting nutrient, for the same reasons it is not limiting in the modern ocean. The ability to fix nitrogen is common among modern anaerobic prokaryotes, and it is thought that this capability developed early in biological evolution (Cloud, 1976; Margulis, 1982; Broda & Peschek, 1983; Fay, 1992; Raymond *et al.*, 2004). We therefore feel justified in neglecting N in this study.

By contrast, P may well have been less available during the Archean than at present. Bjerrum & Canfield (2002) have argued that dissolved P concentrations would have been only 10–25% of their present value as a consequence of adsorption of P by iron oxyhydroxides during BIF deposition. ('BIF' is short for banded iron-formation.) If productivity had been limited by P, as today, it should have been lower by this same amount. We have already suggested that Archean productivity was limited by other factors, specifically the supply of electron donors. To demonstrate this, however, we need to have an estimate for the P-limited productivity rate. Using numbers from Bjerrum & Canfield (2002) gives an estimate of $(4–10) \times 10^{14}$ mol C year^{-1} for Archean NPP.

A comparable estimate of P-limited Archean primary productivity can be obtained by a different argument. Multiplying the P supply value from Tyrrell (1999) by the C:P ratio in organic matter (106 : 1) yields a modern organic carbon burial rate of approximately 10^{13} mol year^{-1}. The burial efficiency of organic carbon in today's ocean is approximately 0.2% (Berner, 1982); thus, modern NPP should be equal to 10^{13} mol year$^{-1} \cdot (0.2\%)^{-1} = 5 \times 10^{15}$ mol year^{-1}, or 60 Gt C year^{-1}. This is roughly consistent with the previous estimate (Prentice *et al.*, 2001). The relative constancy of the ^{13}C content of marine carbonates over time suggests that the burial proportion of organic carbon has not changed greatly since at least 3.0 Ga (Schidlowski *et al.*, 1983; DesMarais, 1997), although Bjerrum & Canfield (2004) have suggested an alternative view (see Discussion section). The burial *efficiency*, however, was probably higher in the distant past because of the absence of O_2 and sulphate from deep water. If the Archean burial efficiency was similar to that of the modern, euxinic Black Sea, approximately 2% (Arthur *et al.*, 1994), then NPP should have been approximately 5×10^{14} mol C year^{-1} or 6 Gt C year^{-1}. The actual burial efficiency in the Black Sea is uncertain and could actually be as low as the open ocean value. We have used the upper limit here. Increasing the burial efficiency of organic carbon by a factor of 10 lowers NPP by this same factor, if burial of organic matter is the dominant sink for P.

Note that our global NPP and CH_4 flux values assume that productivity was equal everywhere. In the modern ocean, this is not the case; some areas of the surface ocean are much more P-rich, and hence much more productive, than others (Fig. 1). If the Archean oceans were similar in this respect to today's oceans, only approximately 30–50% of the surface ocean may have been productive. Thus, our 1D calculations may overestimate NPP and CH_4 production by a factor of 2 or 3.

Despite the fact that P may have been less available during the Archean than today, P would probably *not* have limited productivity in regions where it was available. The next section describes in more detail what the critical electron donors are likely to have been and what types of organisms would have depended on them. A more general discussion of microorganisms and their metabolisms can be found in *Brock Biology of Microorganisms* (Madigan *et al.*, 2002).

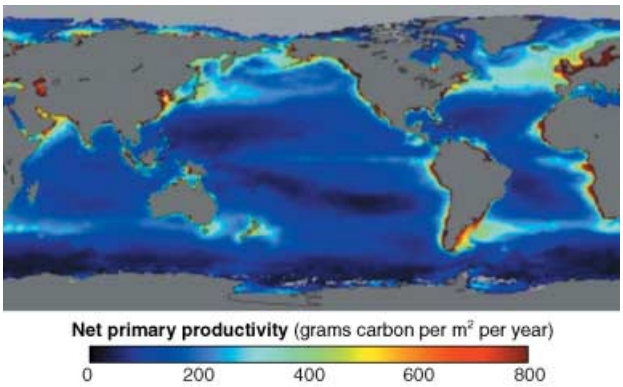

Fig. 1 Spatial distribution of modern marine NPP. (Credit: R. Simmon and W. Gregg, NASA-GSFC. See http://www.gsfc.nasa.gov/goddardnews/20030919/carbon.html).

Anaerobic microbial ecosystems on the Archean Earth

Following other workers who have speculated about life on the anoxic early Earth (e.g. Walker, 1977; DesMarais, 1998), we consider the primary electron donors to have been H_2, CO, H_2S, and Fe^{2+}. Estimates for the rates of supply of each of these compounds will be given in the Results section. The most abundant of these compounds would have been H_2. Hence, we begin by considering plausible H_2-based ecosystems. We discuss CO here as well because, as we will see, CO metabolism probably evolved very early. Otherwise, the atmosphere would have quickly filled up with CO – a process that we term 'CO runaway'. CO-rich early atmospheres are not physically impossible (see, e.g. Kasting, 1990), but they would have been such a rich energy source for life that it seems unlikely that organisms would have allowed them to persist.

H_2- and CO-based metabolism

We first simulated ecosystems in which the primary producers are H_2-using methanogens, H_2-using anoxygenic phototrophs, and CO-consuming acetogens. The corresponding metabolic reactions are, respectively:

$$CO_2 + 4\ H_2 \rightarrow CH_4 + 2\ H_2O \qquad (R1)$$

$$CO_2 + 2\ H_2\ (+ h\nu) \rightarrow CH_2O + H_2O \qquad (R2)$$

$$4\ CO + 2\ H_2O \rightarrow 2\ CO_2 + CH_3COOH \qquad (R3)$$

Phylogenetic sequencing based on protein sequences, as well as whole genome analysis, suggests that H_2-using methanogens evolved sometime during the Archean (House *et al.*, 2003; Battistuzzi *et al.*, 2004). We further assume that these organisms evolved before O_2-producing phototrophs, based on molecular clock estimates (Battistuzzi *et al.*, 2004). As we will show, the early Archean atmosphere likely had ample free H_2, which would have allowed methanogens to thrive in a wide variety of habitats. So, it is certainly plausible that they were extant since very early times.

We also assume, following others (e.g. Walter, 1983; Westall, 2005), that anoxygenic photosynthesis evolved very early. Recently, Tice & Lowe (2004) argued that, based on geochemical and sedimentological data in putative 3.4-Ga microbial mats, anoxygenic phototrophs were likely present in the Archean ocean. Furthermore, Xiong *et al.* (2000) provided a phylogenetic argument that anoxygenic photosynthesis preceded oxygenic photosynthesis. According to their analysis, chlorophyll-a biosynthesis pathways evolved from bacteriochlorophyll-a biosynthesis pathways, and purple bacteria are the earliest diverging lineage of anoxygenic phototrophs. A realistic early Archean ecosystem would probably have contained both H_2-using methanogens and H_2-using phototrophs, along with other photosynthetic organisms that used Fe^{2+} and H_2S as electron donors. Once they had evolved, the phototrophs would likely have dominated productivity in the surface ocean where sunlight was readily available, while the methanogens would have dominated at greater depths. Deep ocean productivity would have been low, however, for reasons discussed below. Hence, Archean primary productivity was probably concentrated in the surface ocean, as it is today,

Most of our simulations also included two groups of secondary organisms – acetogenic bacteria (fermentors) and acetotrophic methanogens – which are dependent on the organic matter produced by the above primary producers, and whose metabolic reactions are, respectively:

$$2\ CH_2O \rightarrow CH_3COOH \qquad (R4)$$

$$CH_3COOH \rightarrow CH_4 + CO_2 \qquad (R5)$$

Because the ocean is deficient in both O_2 and sulphate in our models, most of the organic matter produced by anoxygenic photosynthesis (R2) must have been broken down by these pathways, or by analogous ones involving other fermentation products. Hence, the net result of either R1 or R2 is production of CH_4.

In our model, and probably on the actual Archean Earth as well, this CH_4 flows back into the atmosphere where it is photochemically oxidized to CO. This CO can be further oxidized to CO_2 by reaction with hydroxyl radical, OH ($CO + OH \rightarrow CO_2 + H$); however, the rate at which this reaction occurs is limited by the rate at which OH is produced from photolysis of water vapor ($H_2O + h\nu \rightarrow H + OH$). In many of our simulations, especially those in which H_2 is abundant, CO is produced faster than it can be removed photochemically from the atmosphere; hence, it accumulates without bound unless some other process takes it up. Despite previous assertions to the contrary (Van Trump & Miller, 1973), hydration of CO in the oceans is not fast enough to keep CO from accumulating. This process is analysed in Appendix 3. This phenomenon has been observed in other photochemical modelling studies and has been termed 'CO runaway' (Kasting *et al.*, 1983; Zahnle, 1986).

We assume here that CO did *not* accumulate to extremely high levels because it was a useful substrate and, hence, was consumed by organisms. The enzyme used by such bacteria, CO dehydrogenase, is a bifunctional enzyme that plays a pivotal role in carbon assimilation, both in synthesizing and in degrading acetyl-CoA. It is considered an ancient enzyme and would have been part of the metabolic capacity of prokaryotic ecosystems (Ragsdale, 2004). This could have allowed an efficient and quick metabolic switch to CO for respiration, given the environmental selective pressures (Lindahl & Chang, 2001). Several genera of autotrophic acetogens are known to metabolize CO via R3 (Genthner & Bryant, 1982; Lynd *et al.*, 1982; Kerby & Zeikus, 1983; Kerby *et al.*, 1983). By comparison, methanogens do quite poorly when cultivated on CO; it is far more favourable for them to consume H_2 or acetate (Daniels *et al.*, 1977; O'Brien *et al.*, 1983). Dissolved CO

should not be confused with its hydrated counterpart, formate ($HCOO^-$), which is a good substrate for methanogens. Hydration of CO to give formate is slow at low temperatures, as discussed in Appendix 3. Thus, rapid uptake of CO probably required the existence of acetogens.

Note that the CH_3COOH produced by the primary acetogens (R3) would also have been consumed by the acetotrophic methanogens (R5) to produce CH_4. That overall reaction (R3 + R5) can be written as:

$$4\ CO + 2\ H_2O \rightarrow 3\ CO_2 + CH_4 \qquad (R6)$$

Thus, this reaction sequence effectively balances the photochemical conversion of CH_4 into CO that takes place in the atmosphere.

A simple microbial ecosystem that includes both primary producers and secondary organisms is illustrated in Fig. 2. In the model depicted there, H_2-using methanogens are the primary producers, and the secondary acetogens and methanogens are responsible for anaerobic recycling of the organic matter that the primary methanogens produce. A more realistic diagram that included all the primary producers would be needed to fully represent this part of the model.

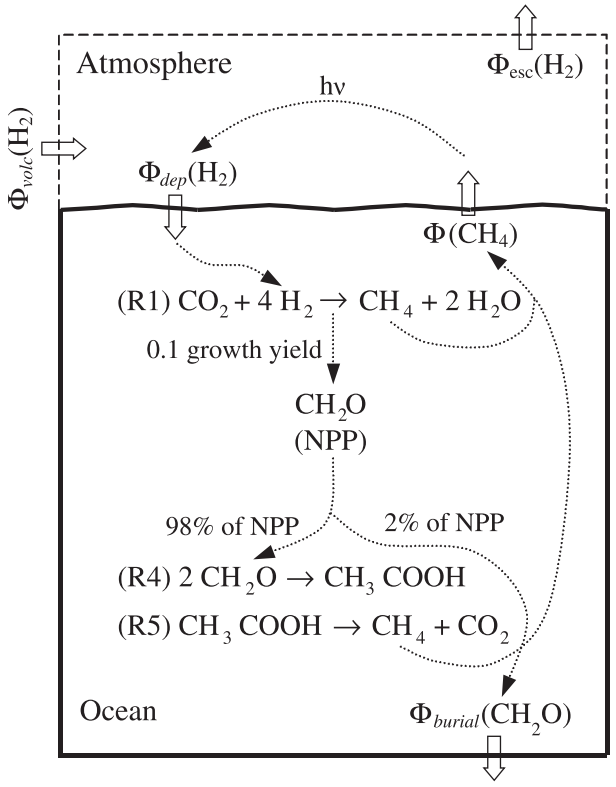

Fig. 2 Diagram of a methanogen-based ecosystem (case 1) showing the relevant biochemical reactions and chemical fluxes (see text for term definitions). As in the text, R1 represents H_2-using methanogens, R4 represents acetogenic bacteria, and R5 represents acetotrophic methanogens. Methanogen growth yield (assimilation:metabolism ratio) is assumed to be 0.1; burial efficiency is assumed to be 2%. The overall balance between $\Phi_{volc}(H_2)$, $\Phi_{esc}(H_2)$, and $\Phi_{burial}(CH_2O)$ determines the total atmospheric H_2 mixing ratio (see next section). Atmospheric H_2 enters the ocean and is converted into organic matter and CH_4 by the biota. This biogenic CH_4 then flows into the atmosphere and is converted back into H_2 (and CO_2) by photolysis.

Sulphur-based metabolism

Sulphur-using organisms were also likely to have been present on the early Archean Earth. Indeed, genomic analysis suggests that elemental sulphur-reducing bacteria might have been the first organisms to evolve (House *et al.*, 2003). Many anoxygenic phototrophs can also use H_2S as a reductant, in place of H_2. We envision this part of the Archean marine ecosystem as being akin to a sulphuretum in which there are two groups of primary producers: elemental sulphur (S_8)-reducing bacteria and H_2S-using anoxygenic phototrophs (e.g. purple and green sulphur bacteria; Madigan *et al.*, 2002). We assume that the sulphur reducers metabolized elemental sulphur via the following reaction:

$$^1/_8\ S_8 + H_2 \rightarrow H_2S \qquad (R7)$$

Most likely, both H_2 and particulate S_8 would have been supplied from the atmosphere and from internal recycling of sulphur within the surface ocean. Little or no recycling of sulphur would probably have occurred in the deep ocean because it was filled with ferrous iron, making sulphide insoluble (Walker & Brimblecombe, 1985). For the H_2S-using phototrophs, we assume the following photosynthetic reaction:

$$CO_2 + 2\ H_2S\ (+ h\nu) \rightarrow CH_2O + 2\ S + H_2O \qquad (R8)$$

H_2S would have been supplied from the atmosphere and from R7.

Our model of the Archean sulphur-based ecosystem is simpler than the real world in that we have not attempted to calculate internal rates of sulphur recycling within the surface ocean. Doing so would require kinetic data from sulphureta, and we have not been able to locate such information. Thus, the productivity of our sulphur-based ecosystem is limited by the atmospheric deposition fluxes of H_2, S_8, and H_2S, which are in turn limited by the H_2 and SO_2 outgassing rates. We note that H_2S-using phototrophs would likely *not* have thrived in regions where ferrous iron was being upwelled. There, the supply of iron would have vastly exceeded the supply of sulphur, thus sulphur would have been rapidly removed by pyrite formation. Upwelling regions comprise only a small fraction of the surface ocean, though, and so much of the Archean surface ocean may have supported an ecosystem based on R7 and R8.

Iron-based metabolism

A third source of reducing power for fixing CO_2 photosynthetically is ferrous iron, Fe^{2+}. This photoautotrophic reaction is conventionally written as follows:

$$4\,Fe^{2+} + CO_2 + 11\,H_2O\,(+h\nu) \rightarrow 4\,Fe(OH)_3 + CH_2O + 8\,H^+ \quad (R9)$$

Such iron-oxidizing phototrophs could have been important primary producers in upwelling regions of the Archean ocean. These anoxygenic phototrophs are believed to have played an important role in the formation of at least some Precambrian banded iron-formations, or BIFs (Ehrenreich & Widdel, 1994; Konhauser *et al.*, 2002; Kappler & Newman, 2004). BIFs are sedimentary rock deposits, some of which contain oxidized iron compounds despite having formed under an anoxic atmosphere. Geologists have argued for the last 50 years or more about exactly how the iron in BIFs became oxidized. We will not attempt to resolve that debate here. We simply concern ourselves with deriving estimates for how productive Fe-based metabolism could have been under completely anoxic conditions. These estimates are provided in the Results section.

Overview of model scenarios

The timeline for the evolution of Archean organisms remains uncertain. In this study we have taken a reductionist approach and considered five simplified case scenarios with different combinations of the organisms described above. These are as follows. Case 1: chemotrophic methanogens, acetogenic bacteria, and acetotrophic methanogens (R1, R4, and R5, respectively). Case 2: same three organisms as in Case 1, plus CO-consuming acetogens (R3). Case 3: H_2-using anoxygenic phototrophs, CO-consuming acetogens, acetogenic bacteria, and acetotrophic methanogens (R2, R3, R4, and R5, respectively). Case 4: elemental sulphur reducers and H_2S-using anoxygenic phototrophs (R7 and R8, respectively). Case 5: Fe^{2+}-oxidizing phototrophs (R9). Cases 1–4 all require numerical simulations with the coupled photochemical-ecosystem model, whereas Case 5 does not.

MODEL DESCRIPTION

In the previous section we described the types of organisms that we consider to have been important components of the Archean biosphere. To make meaningful estimates of rates of primary production and trace gas fluxes, though, we need a detailed physical model of the atmosphere and surface ocean. This section provides those details.

Ecosystem model

In most of the anaerobic ecosystems that we are considering, primary productivity would have been limited by the downward flux of H_2, CO, S_8, and H_2S across the atmosphere–ocean interface. Likewise, the flux of CH_4 into the atmosphere would have been limited by its rate of upward transport through this same interface. To evaluate these fluxes, we adopted the stagnant boundary layer model (Liss & Slater, 1974). This approach presumes that there is a thin layer at the top of the ocean surface through which the gas must pass by molecular diffusion (see Fig. 3). In reality, the atmosphere–ocean interface is more complex, with wave-breaking, bubble formation, etc.; however, the stagnant boundary layer approach allows us to bypass these complications in a semiempirical manner. By a procedure that is well known to marine geochemists, the thickness of the stagnant layer ($z_{film} \approx 40\ \mu m$) is determined empirically, either from measurements of natural ^{14}C in the atmosphere and surface ocean or from tracer distributions in wind tunnel experiments. (See discussion in Broecker & Peng, 1982.) We assume that the rates at which any gas can flow through the atmosphere–ocean interface is limited by its piston velocity. The piston velocity is the rate at which a dissolved gas would be expelled from the water column by a piston moving upwards at constant velocity. In this approach, the flux of a gas is proportional to the product of its piston velocity and its concentration gradient between the top and the bottom of the stagnant boundary layer. At the top of the layer, the gas concentration is in Henry's Law equilibrium with the atmosphere; at the bottom it is equal to the dissolved gas concentration in the surface ocean. Under these assumptions, the molecular flux of a gas X across the atmosphere–ocean interface can be expressed mathematically as:

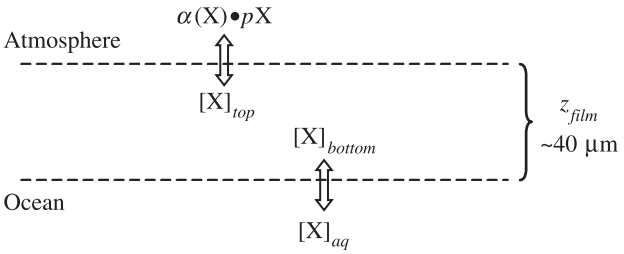

Fig. 3 The stagnant boundary layer model. The flux of gas X across the atmosphere–ocean interface is equal to the product of its piston velocity ($v_p(X) = K_{diffusion}(X)/z_{film}$) and its concentration gradient between the top and bottom of the boundary layer ($[X]_{top} - [X]_{bottom}$).

$$\Phi(X) = \nu_p(X) \cdot (\alpha(X) \cdot pX - [X]_{aq}) \cdot C, \quad (1)$$

where $\nu_p(X)$ = piston velocity of species X = $K_{diff}(X)/z_{film}$,
$K_{diff}(X)$ = thermal diffusivity of X,
$\alpha(X)$ = solubility of X (i.e. the Henry's law coefficient),
pX = partial pressure of X (in bar),
$[X]_{aq}$ = dissolved concentration of X (in mol L^{-1}), and
$C = 6.02 \times 10^{20}$ molecules cm^{-3} mol^{-1} L (units conversion factor).

Parameter values for several key gases at 25 °C are shown in Table 1. As explained in the Results section, the temperature dependence in our model is fairly weak; thus, for convenience we use these 25 °C parameter values in all of our simulations.

Table 1 Solubilities, thermal diffusivities, and piston velocities for relevant gases*

Gas	Solubility†	Diffusivity‡	Piston velocity§
H_2	7.8×10^{-4}	5.0×10^{-5}	1.3×10^{-2}
CH_4	1.4×10^{-3}	1.8×10^{-5}	4.5×10^{-3}
CO	1.0×10^{-3}	1.9×10^{-5}	4.8×10^{-3}
H_2S	10^{-1}	1.4×10^{-5}	3.4×10^{-3}

*Data from NIST Chemistry WebBook 2003 & Lide 2000; all values at 25 °C.
†In mol L^{-1} bar^{-1}.
‡In cm^2 s^{-1}.
§In cm s^{-1}, assuming film thickness of 40 μm.

The kinetic constraint imposed by this stagnant boundary layer approach requires that dissolved gas concentrations in the surface ocean be in disequilibrium with the atmosphere. For example, because H_2 needs to flow downward from the atmosphere into the ocean, the dissolved H_2 concentration in the surface ocean, $[H_2]_{aq}$, must be less than the dissolved H_2 concentration at the top of the boundary layer, $\alpha(H_2) \cdot pH_2$. The opposite is true for CH_4 because it is flowing upward.

Atmosphere model

The atmospheric photochemistry model is a modified version of the one described in detail by Pavlov *et al.* (2001a). It simulates an anoxic Archean atmosphere in which surface O_2 concentrations are approximately 10^{-12} of the present atmospheric level (PAL). It is one-dimensional (in altitude) and contains 73 chemical species involved in 359 reactions; its grid height is 100 km. The solar zenith angle is fixed at 50°, and a two-stream approach is used for the radiative transfer.

Assessment of the redox balance is a crucial part of this and all anoxic atmosphere models. We did this by keeping track of the atmospheric hydrogen budget, i.e. the flow of electrons into and out of the system (Appendix 1). The hydrogen budget can be subdivided into two separate components. The first is the overall balance for the combined atmosphere–ocean system between volcanic outgassing of H_2 (and other reduced gases), H_2 escape to space, and burial of organic carbon. The second is the balance between production and loss of oxidized and reduced species for the atmosphere by itself. Ignoring the atmospheric balance for now, we can express the overall hydrogen balance mathematically as

$$\Phi_{volc}(H_2) = \Phi_{esc}(H_2) + 2\,\Phi_{burial}(CH_2O). \quad (2)$$

In practice, $\Phi_{volc}(H_2)$ is calculated recursively – we first set it equal to $\Phi_{esc}(H_2)$, then we factor in the $\Phi_{burial}(CH_2O)$ term with each subsequent iteration until the model converges. The next paragraph describes how we calculate $\Phi_{esc}(H_2)$; the next subsection below describes how $\Phi_{burial}(CH_2O)$ is derived. The coefficient of 2 in Eqn 2 arises because 2 mol of H_2 are needed to reduce 1 mol of CO_2 to organic carbon: $CO_2 + 2\,H_2 \rightarrow CH_2O + H_2O$. Similar stoichiometric coefficients arise in the other redox relations, as described in Appendix 1. Equation 2 states that the net flux of reducing power into the atmosphere–ocean system must equal the net flux out. Three other terms have been neglected here: (i) the difference between the Fe^{2+} upwelling rate and the BIF formation rate should appear on the left-hand side of Eqn 2; (ii) sulphate that reacts with reduced iron on the seafloor should also appear on the left; and (iii) the burial of pyrite should appear on the right. The terms involving sulphur are small, according to the numbers assumed here, and have hence been ignored. The iron flux is significant and would serve to increase the amount of H_2 supplied to the atmosphere–ocean system, leading to slightly higher atmospheric H_2 and CH_4 concentrations than predicted here. The uncertainties are small, however, compared to those described immediately below.

In all of our models, the escape rate of H_2 to space is assumed to be limited by the rate of diffusion of H_2 through the homopause at approximately 100 km (but see below). This diffusion-limited escape flux is calculated as follows (Hunten, 1973; Walker, 1977):

$$\Phi_{esc}(H_2) \approx 2.5 \times 10^{13} \cdot f_{tot}(H_2) \text{ molecules cm}^{-2}\text{ s}^{-1}, \quad (3)$$

where

$$f_{tot}(H_2) = f(H_2) + 2\,f(CH_4) + f(H_2O) + \ldots \quad (4)$$

is the sum of the mixing ratios of all H_2-bearing atmospheric constituents above the tropopause, weighted by the amount of hydrogen they contain. We keep track of the hydrogen budget in terms of H_2 molecules, rather than H atoms. Henceforth, we will also follow standard atmospheric chemists' notation and omit the word 'molecules' from the flux units. In accordance with climate modelling results (e.g. Kasting & Ackerman, 1986; Pavlov *et al.*, 2000) we assume that the Archean atmosphere was dry above the tropopause, as it is today. Hence, Eqn 4 is simplified to:

$$f_{tot}(H_2) \approx f(H_2) + 2\,f(CH_4). \quad (5)$$

The modern volcanic H_2 outgassing rate is approximately 5×10^{12} mol $year^{-1}$, or approximately 2×10^{10} cm^{-2} s^{-1} (Holland, 2002). During the Archean the H_2 outgassing rate was probably higher than it is today and, importantly, H_2 escape may have proceeded at less than the diffusion limit (Tian *et al.*, 2005; see also the Discussion section). Thus, using $f_{tot}(H_2)$ as our independent variable, we have performed calculations over a range of different total hydrogen mixing ratios, including ones much greater than our minimalist assumptions would predict. The effect of CH_4 on Archean climate would have been greatest if hydrogen escape was slow.

Coupled atmosphere–ecosystem model

Most of the complexity in our model is related to our simulations of H_2-based ecosystems, so we describe that part of the model first. Our sulphur- and iron-based ecosystem models are simple by comparison because no recycling of these compounds is assumed to occur.

To determine the global biogenic CH_4 flux and NPP of our H_2-based coupled atmosphere–ecosystem models (Cases 1–3), we first set the appropriate lower boundary conditions on the three main gases of interest: H_2, CO, and CH_4. For our methanogen-based ecosystems (Cases 1 and 2), we used fixed mixing ratio lower boundary conditions for both CH_4 and H_2, subject to the constraint that their weighted sum equalled $f_{tot}(H_2)$ (Eqn 5). When these boundary conditions are applied, the photochemical model automatically determines the (upward or downward) flux of each gas at the surface, based purely on the model chemistry and conservation of mass. To incorporate the ecology of H_2-using methanogens in the ecosystem model, we used the free energy form of the Nernst equation and assumed that the methanogens would consume dissolved H_2 until they obtained 30 kJ mol^{-1} from reaction R1. This is the approximate Gibbs free energy change, ΔG, needed to synthesize 1 mol of ATP. (See Appendix 2 for details.) This type of assumption is standard in modelling of anaerobic ecosystems (see, e.g. Zinder, 1993; Kral *et al.*, 1998; Kasting *et al.*, 2001). The precise value of ΔG at which H_2 uptake is presumed to cease varies from one study to the next and may be as low as 10–20 kJ mol^{-1} (Conrad, 1999). Lower ΔG values would correspond to slightly higher methane fluxes than found here. A sensitivity test, described in the Results section, shows that decreasing ΔG has a relatively small effect on calculated methane fluxes and NPP.

Based on laboratory studies of H_2-using methanogens (Schönheit *et al.*, 1980; Fardeau & Belaich, 1986; Morii *et al.*, 1987), we assume that these organisms assimilate 1 mol of CO_2 into biomass for every 10 mol they metabolize; thus, the organic matter production rate (NPP) is 10 times lower than the CH_4 production rate. The actual ratio of assimilation to metabolism, referred to as the 'growth yield', is variable in laboratory studies. The 1:10 ratio assumed here is reasonable for substrate-limited growth, which is what occurs in the model when primary production is limited by H_2. A higher growth ratio would have little effect on the predicted methane flux but would increase NPP at a given value of $f_{tot}(H_2)$. To calculate $\Phi_{burial}(CH_2O)$, we multiply NPP by an assumed organic carbon burial efficiency, f_B. We use the modern value of 0.2% (Berner, 1982) as a lower limit on f_B and we use 2% as an upper limit (see Fig. 2). The latter value corresponds to the organic carbon burial efficiency estimated for the Black Sea (Arthur *et al.*, 1994), which is a modern anoxic ocean basin. The calculated values of $\Phi_{burial}(CH_2O)$ are then used in Eqn 2 to compute the relationship between volcanic outgassing rates and the total hydrogen mixing ratio of the atmosphere. Note that in this formulation, the recycling efficiency is given by $1\text{-}f_B$, and thus the internal CH_2O recycling rate can be calculated as $[1\text{-}f_B] \cdot$ NPP. However, only the CH_2O burial rate affects the overall redox balance.

For Cases 1 and 2, the solution is found as follows: We first fix the atmospheric CH_4 and H_2 mixing ratios, as described above, and determine the upward flux of CH_4 from the photochemical model. (The upward CH_4 flux is equal to the net photochemical destruction rate of CH_4 in the model atmosphere.) Next, we use the stagnant boundary layer model (Eqn 1) to find the dissolved CH_4 concentration in the surface ocean. Then, we use the Nernst equation (Eqn A2.1) to derive the dissolved H_2 concentration, and we calculate the H_2 deposition flux from the stagnant boundary layer model. This procedure yields an H_2 flux, $\Phi_{eco}(H_2)$, that can be compared with the H_2 deposition flux, $\Phi_{dep}(H_2)$, computed by the photochemical model. In general, these two H_2 fluxes do not agree, and so the procedure is repeated using different atmospheric H_2 and CH_4 mixing ratios until a self-consistent solution is obtained (Fig. 4). The point where $\Phi_{eco}(H_2)$ and $\Phi_{dep}(H_2)$ intersect in Fig. 4 represents a unique solution to the coupled photochemical-ecosystem model for a given value of $f_{tot}(H_2)$. This unique solution could in principle be found more economically by allowing the surface H_2 and CH_4 mixing ratios to adjust during the calculation, but we used the more cumbersome procedure described above to maintain strict control over this relatively complex coupled model.

For Case 3, we assume that the anoxygenic phototrophs would have consumed H_2 as fast as it flowed into the ocean, as they are not limited by the same free energy requirements as the methanogens. Thus, rather than fixing the H_2 mixing ratio, we fix the H_2 deposition velocity at its maximum allowable value, 2.4×10^{-4} cm s^{-1}. (See the ensuing discussion of CO deposition for how this value is derived.) The photochemical

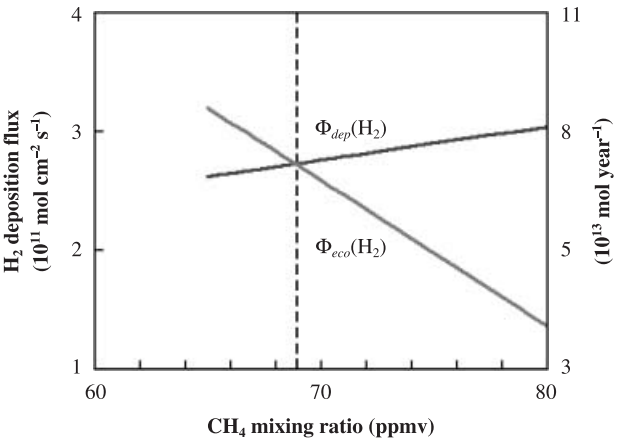

Fig. 4 H_2 deposition fluxes from the ecosystem model [$\Phi_{eco}(H_2)$] and the photochemistry model [$\Phi_{dep}(H_2)$] as a function of CH_4 concentration for $f_{tot}(H_2)$ = 200 ppmv. The intersection between the two curves corresponds to the steady-state concentration of CH_4. The CO_2 mixing ratio was kept constant at 2500 ppmv.

model then calculates both the H_2 deposition flux and the H_2 mixing ratio. In this case, the NPP is simply equal to $^1/_2$ of the H_2 deposition flux, based on the stoichiometry of reaction R2 (i.e. 2 mol of H_2 are used to produce 1 mol of CH_2O). As with Cases 1 and 2, we calculate $\Phi_{burial}(CH_2O)$ by multiplying NPP by the organic carbon burial efficiency, f_B.

The lower boundary condition on CO is also important. For the two cases in which we include CO-consuming acetogens (Cases 2 and 3), we initially assumed a fixed CO mixing ratio. This mixing ratio was then adjusted iteratively to find a self-consistent solution, as was done for H_2 in the methanogen-based ecosystems. However, we found that the dissolved CO concentration was always negligible compared to the CO concentration at the top of the boundary layer (see Eqn 1). The reason is that CO consumption is so thermodynamically favourable that acetogens pull its dissolved concentration down to extremely low values, at least under our assumption of fixed ΔG for R3. Thus, the downward CO deposition flux is essentially equal to the maximum value allowed by the stagnant boundary layer model. This allows us to use a fixed deposition velocity lower boundary condition for CO, calculated as follows:

$$v_{dep}(\mathrm{CO}) = \frac{v_p(\mathrm{CO}) \cdot a(\mathrm{CO}) \cdot C}{n_{air}}, \qquad (6)$$

where n_{air} is the total number density of air molecules. The value of this (maximum) CO deposition velocity is 1.2×10^{-4} cm s^{-1}. This value is about half that of H_2 because of the lower thermal diffusivity of CO in solution (Table 1). The photochemical model then automatically calculates both the deposition flux and the mixing ratio of CO.

For our sulphur-based ecosystem (Case 4), we first set $f_{tot}(H_2)$ = 800 ppmv, i.e. the 'prebiotic' value derived from assuming the modern volcanic H_2 outgassing rate and H_2 escape rate and neglecting organic carbon burial in Eqn 2. We used fixed CH_4 and H_2 mixing ratios and assumed the constraint on $f_{tot}(H_2)$ imposed by Eqn 5. We then lowered CH_4 levels (and correspondingly, raised H_2 levels) as much as allowable in the photochemical model in order to simulate an ecosystem in which methanogens had not yet evolved. Recall from the previous sections that sulphur metabolism appears to have preceded all other metabolisms. In addition, using values from the NIST Chemistry WebBook and applying the Gibbs equation ($\Delta G = \Delta H - T\Delta S$, where ΔH = enthalpy change, T = temperature, and ΔS = entropy change) to R7, we found that $\Delta G^0 = -33.3$ kJ mol^{-1} for R7. Then, using model-calculated values of pH_2S and pH_2, we applied the Nernst equation to the same reaction and determined that, on average, our sulphur reducers obtain approximately 60 kJ mol^{-1} from R7; thus, there are effectively no thermodynamic barriers on their metabolism. So, rates of productivity in our sulphur-based ecosystem were controlled only by the downward flux of sulphur species from the atmosphere, a kinetic constraint.

Note that the bulk of both the sulphur- and H_2-based productivity should have occurred in the *surface* ocean (the top approximately 100 m, corresponding to the wind-mixed/photic zone). The productivity of the deep ocean should have been much lower because the downward flux of H_2 would have been slower and because sulphur would have been consumed by reaction with ferrous iron. The H_2 supply to the deep ocean would have been slower than the supply to the surface ocean by the ratio of the piston velocity to the surface-deep ocean mixing velocity. The former is approximately 1.3×10^{-2} cm s^{-1} (Table 1), while the latter is approximately 1.2×10^{-5} cm s^{-1}, based on an average ocean depth of 4 km and a deep ocean turnover time of 1000 year. Thus, on average, H_2 would have been supplied to the deep ocean approximately 1000 times more slowly, implying that deep ocean H_2-based productivity was lower than surface productivity by this same factor.

RESULTS

As anticipated in the previous sections, we present the results of our calculations in reductionist fashion, analysing one type of ecosystem at a time and adding additional complexity when needed. In reality, all of the anaerobic metabolisms discussed herein would have been represented in a single complex ecosystem. But that whole, complex ecosystem can be best understood by examining one component at a time.

Case 1: Methanogen-based ecosystem

Primary production by R1 and recycling by R4 and R5 were considered here. Figure 4 shows an example of a self-consistent solution for this system for prescribed values of $f_{tot}(H_2)$ = 200 ppmv and $f(CO_2)$ = 2500 ppmv. This CO_2 mixing ratio is less than one would need climatically to offset the faint young Sun; however, it will become apparent in a moment why we started at these relatively low total hydrogen and CO_2 concentrations. The calculated CH_4 and H_2 concentrations for this case are approximately 70 ppmv and approximately 60 ppmv, respectively. This CH_4 concentration is approximately 40 times higher than the modern CH_4 concentration of 1.7 ppmv, indicating that methane should have been an important atmospheric constituent even for this minimalist case.

Figure 5(A) shows the vertical mixing ratio profiles for H_2, CH_4, and CO for this solution. The CH_4 mixing ratio is relatively high near the surface but decreases in the middle and upper atmosphere, while the opposite is true for H_2. This is because methanogens draw down H_2 near the surface to make CH_4; then at higher altitudes CH_4 is converted back to H_2 and CO_2 (or CO) by photolysis and subsequent photochemical reactions.

The corresponding H_2 and CH_4 fluxes are shown in the first row of Table 2. The modern global biogenic CH_4 flux is approximately 600 Tg CH_4 $year^{-1}$, or approximately 3.6×10^{13} mol $year^{-1}$ (Prather *et al.*, 2001). By comparison, the CH_4 flux

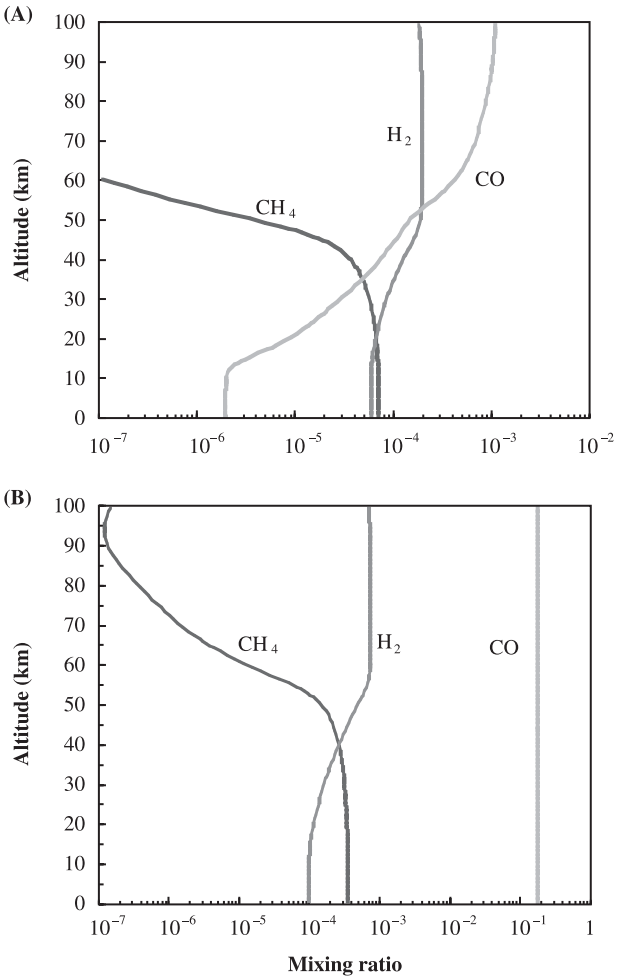

Fig. 5 Vertical mixing ratio profiles of H_2, CH_4, and CO in our Case 1 ecosystem for $f_{tot}(H_2)$ = (a) 200 ppmv and (b) 800 ppmv. The CO_2 mixing ratio was fixed at 2500 ppmv for both cases. In the absence of a biotic sink, CO can quickly accumulate to very high levels in a methanogenic ecosystem.

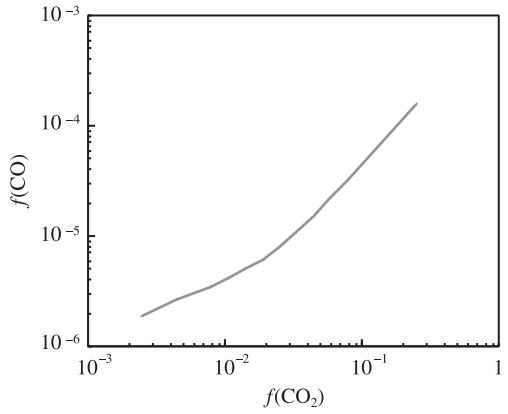

Fig. 6 Surface mixing ratio of CO as a function of CO_2 in the Case 1 ecosystem for $f_{tot}(H_2)$ = 200 ppmv. As is the case when the CH_4 mixing ratio is increased (Fig. 5), CO can rapidly increase with increasing CO_2 if there are no CO-consuming biota.

from our $f_{tot}(H_2)$ = 200 ppmv model run is approximately 1.9×10^{13} mol year^{-1}, or just over half of the modern value. Higher values of $f_{tot}(H_2)$ yield CH_4 fluxes equal to or greater than the modern flux. In the anoxic Archean atmosphere, these fluxes would have supported CH_4 levels between approximately 70–350 ppmv for this case (Table 2). For a solar constant equal to 80% of the present value (the expected value at 2.7 Ga), these CH_4 levels would have led to mean global surface temperatures slightly lower than today's value of 288 K (Pavlov *et al.*, 2000). The higher CH_4 concentration in the Archean atmosphere, compared to today, is a consequence of its longer photochemical lifetime.

At high values of $f_{tot}(H_2)$ this Case 1 ecosystem yields very high CO concentrations (Fig. 5B). The CO concentration in this simulation is approximately 20% by volume. Still higher values of $f_{tot}(H_2)$ lead to CO runaway. CO runaway can also result from increases in CO_2, as photolysis of CO_2 is another CO source (Fig. 6). The cases described below presume that the ability to metabolize CO would have evolved quickly, thereby keeping CO levels relatively low.

We have performed two simple sensitivity tests to determine the effects of changing two of our model input parameters. First, we decreased ΔG from –30 kJ mol^{-1} to –10 kJ mol^{-1} for the H_2-using methanogens. This increased both the H_2 deposition flux and the CH_4 flux, but only slightly (approximately 1%). The reason our results are so insensitive to ΔG is that, as described in Appendix 2, ΔG^0 = –131 kJ mol^{-1} at 25 °C; thus, the concentration gradient of H_2 within the stagnant boundary layer (see Eqn 1) is largely unaffected by a 20 kJ mol^{-1} change in ΔG, because dissolved H_2 changes relatively little (see Eqn A2.3). Second, we increased the model atmosphere and ocean temperatures by 25 °C, and likewise found only minor (1–10%) changes in the fluxes and mixing ratios of interest.

Case 2: Methanogen–acetogen ecosystem

Here, R3 was added to the system from Case 1. For this case, as well as for Case 3, we increased the CO_2 mixing ratio to 25 000 ppmv (2.5%) in order to simulate more climatically plausible conditions for the early Archean, and we ran the coupled model using six different levels of $f_{tot}(H_2)$: 200, 500, 800, 2000, 5000, and 10 000 ppmv. (Note: As a consequence of using fixed $v_{dep}(H_2)$ as opposed to fixed $f(H_2)$ for Case 3, our values of $f_{tot}(H_2)$ in that case differ slightly from the six values listed here; however, these discrepancies are small and have little effect on our results.) For both of these cases, we determined the downward CO flux by applying the fixed deposition velocity lower boundary condition (Eqn 6) to the photochemical model. Figure 7 shows calculated mixing ratio profiles of H_2, CO, and CH_4 for three Case 2 simulations with total hydrogen mixing ratios ranging from 200 ppmv to

Table 2 Fluxes, mixing ratios, and NPP values for the Case 1 and Case 3 ecosystems*

Case 1									
$f_{tot}(H_2)$	$\Phi_{volc}(H_2)$	$f(H_2)$	$f(CH_4)$	$[H_2]$	$[CH_4]$	$\Phi_{dep}(H_2)$	$\Phi(CH_4)$	NPP†	NPP§
200	5×10^9	60	70	1.29×10^{-8}	1.24×10^{-7}	2.76×10^{11}	6.95×10^{10}	6.95×10^9	1.86×10^{12}
500	1.25×10^{10}	100	200	1.64×10^{-8}	3.22×10^{-7}	4.44×10^{11}	1.14×10^{11}	1.14×10^{10}	3.05×10^{12}
800	2×10^{10}	100	350	1.87×10^{-8}	5.40×10^{-7}	5.20×10^{11}	1.35×10^{11}	1.35×10^{10}	3.61×10^{12}
Case 3									
$f_{tot}(H_2)$	$\Phi_{volc}(H_2)$	$f(H_2)$	$f(CH_4)$	$[H_2]$**	$[CH_4]$	$\Phi_{dep}(H_2)$	$\Phi(CH_4)$	NPP‡	NPP§
200	6.32×10^9	22.2	83	–	1.30×10^{-7}	1.32×10^{11}	3.75×10^{10}	6.98×10^{10}	1.86×10^{13}
500	1.45×10^{10}	33	227	–	3.42×10^{-7}	1.96×10^{11}	6.55×10^{10}	1.05×10^{11}	2.79×10^{13}
800	2.25×10^{10}	42	372	–	5.54×10^{-7}	2.45×10^{11}	8.93×10^{10}	1.31×10^{11}	3.50×10^{13}
2000	5.37×10^{10}	62.1	960	–	1.40×10^{-6}	3.69×10^{11}	1.53×10^{11}	2.00×10^{11}	5.34×10^{13}
5000	1.30×10^{11}	88	2442	–	3.50×10^{-6}	5.24×10^{11}	2.27×10^{11}	2.85×10^{11}	7.61×10^{13}
10000	2.56×10^{11}	108	4927	–	7.00×10^{-6}	6.45×10^{11}	2.80×10^{11}	3.51×10^{11}	9.38×10^{13}

*$\Phi_{volc}(H_2)$ is the outgassing flux of H_2, and $\Phi(CH_4)$ is the biogenic CH_4 efflux from the ocean. All fluxes are in units of molecules cm^{-2} s^{-1}, mixing ratios are in ppm by volume, and $[H_2]$ and $[CH_4]$ are in mol L^{-1}.

**$[H_2]$ for Case 3 is effectively zero by default, because we assume H_2-using phototrophs consume H_2 as soon as it is deposited into the ocean (see previous section).

†NPP in molecules C cm^{-2} s^{-1}, where NPP = $^1/_{10}$ $\Phi(CH_4)$.

‡NPP in molecules C cm^{-2} s^{-1}, where NPP = $^1/_2$ $\Phi_{dep}(H_2)$ + $^1/_{10}$ $\Phi(CH_4)$.

§NPP in mol C $year^{-1}$, where 1 mol $year^{-1}$ = 0.00374 molecules cm^{-2} s^{-1}.

5000 ppmv. The inclusion of the CO-consuming acetogens keeps CO mixing ratios relatively low (approximately 10^{-4} or below) in all cases. H_2 and CH_4 concentrations increase with increasing $f_{tot}(H_2)$, subject to the constraints imposed by Eqn 5 and the thermodynamically controlled marine ecosystem.

Additional simulations for Case 2 are reported below under Case 3. We have combined them with Case 3 because the results are surprisingly similar at a particular value of $f_{tot}(H_2)$. (The likely value of $f_{tot}(H_2)$, however, depends on which case is being considered. See Discussion.) This, as we will see, is a pleasant surprise from a modelling standpoint because it makes it easier to analyse the results. We will explain the reasons for this as we go along.

Case 3: Anoxygenic phototroph–acetogen ecosystem

Here, we replaced R1 (H_2-based methanogenesis) with R2 (H_2-based anoxygenic photosynthesis). R3, R4, and R5 were also included. As shown in Fig. 8 and Table 2, the H_2, CO, and CH_4 surface fluxes calculated for this system all increased with increasing $f_{tot}(H_2)$. The fluxes for Cases 2 and 3 were nearly indistinguishable, so Fig. 8 represents both scenarios. The CH_4 flux ranged from $(1–8) \times 10^{13}$ mol $year^{-1}$, which corresponds to approximately $^1/_3$ to 2.3 times the present CH_4 flux. This result is also nonintuitive. There is no a priori reason to expect that a completely anaerobic marine Archean biosphere should generate roughly the same methane flux as the present aerobic terrestrial biosphere. This result is a complete coincidence, albeit a reassuring one for other Archean atmosphere modelers who have made this assumption without having any particularly good basis for it (e.g. Pavlov *et al.*, 2000, 2001a).

The surface mixing ratios of H_2, CO, and CH_4 for Case 3 are shown in Fig. 9. Note that the ratio of CH_4:H_2 increases with increasing $f_{tot}(H_2)$. This is because 4 mol of H_2 are required to generate 1 mol of CH_4, whether by R1 or by R2 (twice) followed by R4 and R5. The calculated CH_4:H_2 ratio *does* depend slightly on the assumed ecosystem model (Fig. 10). This ratio is higher for the Case 3 ecosystem because the anoxygenic photosynthesizers are not limited by the same thermodynamic free energy constraints as are the H_2-using methanogens; hence, they are able to draw H_2 concentrations down to lower values. Calculated CH_4:H_2 ratios for Case 2 range from approximately 2–35, whereas for Case 3 they range from approximately 4–45. These values may be compared with the ratios of 10–20 predicted by Kasting *et al.* (2001) based on thermodynamic arguments alone. Evidently, kinetic limitations (the transfer rate of H_2 and CH_4 through the atmosphere–ocean interface) suppress the CH_4:H_2 ratio for $f_{tot}(H_2) \leq 2000$ ppmv. For Case 3, the higher CH_4:H_2 ratios found at higher values of $f_{tot}(H_2)$ are a consequence of the greater drawdown of H_2 by the anoxygenic phototrophs. For Case 2, the increasing CH_4:H_2 ratios result from the assumed relatively high concentration of CO_2, which suppresses dissolved H_2 by pushing R1 further to the right. By contrast, the Kasting *et al.* (2001) model had lower CO_2 concentrations at high values of $f_{tot}(H_2)$ because those calculations assumed a fixed surface temperature: CO_2 was inversely correlated with CH_4 because both gases contribute to the greenhouse effect.

These results suggest that once methanogens of any type evolved on Earth, they should have converted most of the available H_2 into CH_4. This is not a new idea. This conclusion was reached more than 25 years ago by Walker (1977) based on purely heuristic arguments. We have simply quantified his

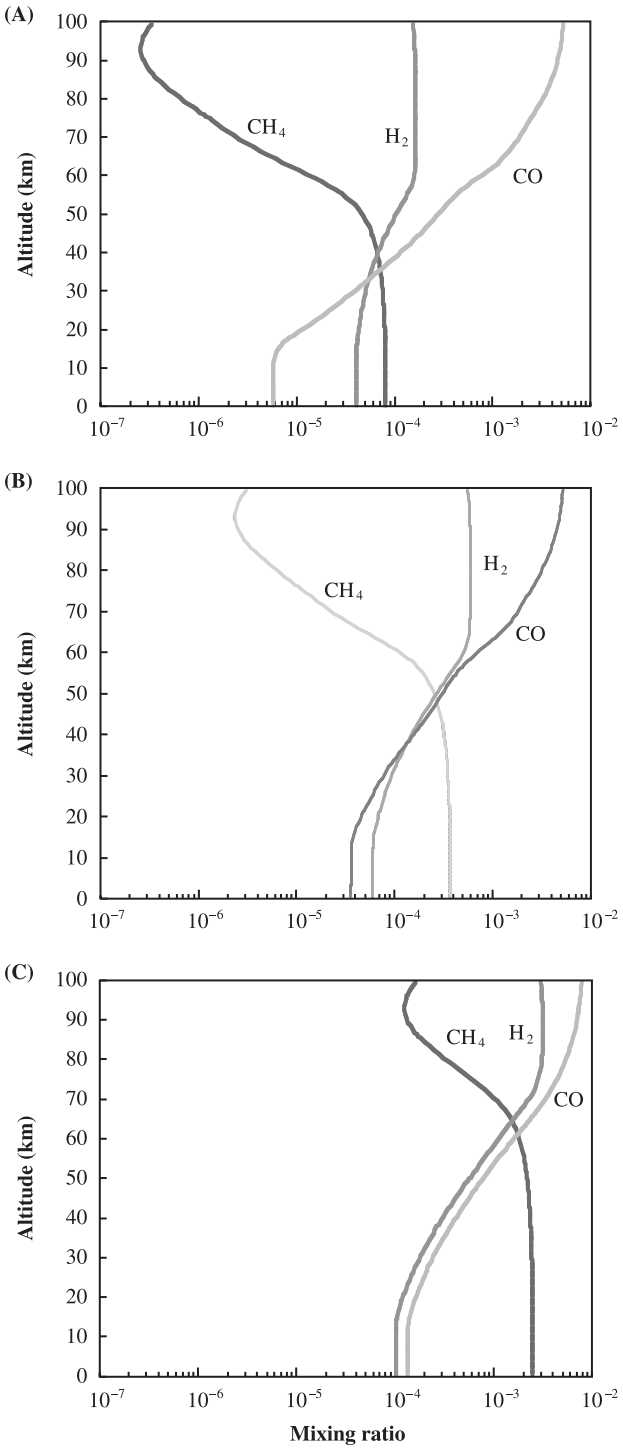

Fig. 7 Vertical mixing ratio profiles of H_2, CH_4, and CO in our Case 2 ecosystem for $f_{tot}(H_2)$ = (A) 200 ppmv, (B) 800 ppmv, and (C) 5000 ppmv. The level of CO_2 was kept constant at 25 000 ppmv (2.5%) for each case.

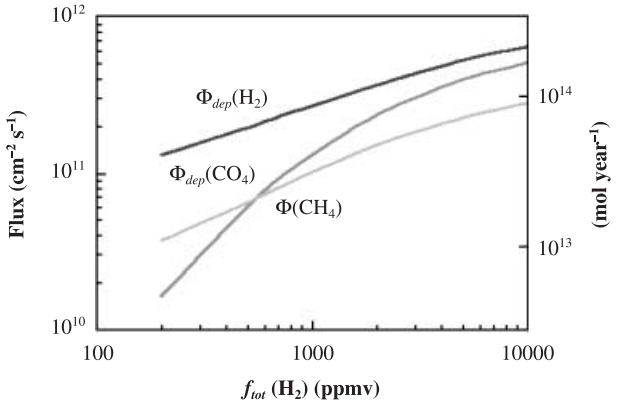

Fig. 8 Surface fluxes of H_2, CO, and CH_4 as a function of $f_{tot}(H_2)$ for the Case 3 ecosystem. The Case 2 system produced essentially identical values for these fluxes, thus it is not shown here.

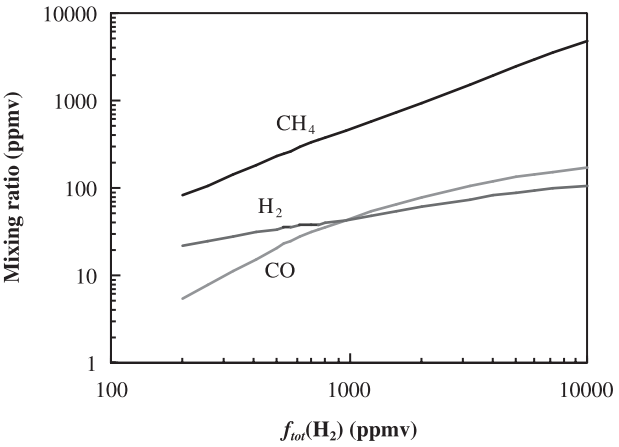

Fig. 9 Surface H_2, CH_4, and CO mixing ratios as a function of $f_{tot}(H_2)$ for Case 3. Results for Case 2 (not shown) were similar.

original prediction. That being said, it should be clear from our analysis that predicting the actual CH_4:H_2 ratio in the Archean atmosphere would require knowledge of the surface temperature and greenhouse effect, along with a good climate model to deduce how much of this was due to CO_2 and how much to CH_4. We have presented a methodology for calculating CH_4 fluxes and CH_4:H_2 ratios, but obtaining accurate answers requires that one be able to better constrain these parameters.

Our Case 2 and Case 3 ecosystems are remarkably similar in terms of the amount of methane that they generate, again for a given value of $f_{tot}(H_2)$. Net primary productivity for the two ecosystems is quite different, however, as shown in Fig. 11. NPP is a factor of 13–20 larger in Case 3 than in Case 2. This is because NPP for Case 2 is equal to 1/10th of the CH_4 production rate, whereas NPP for Case 3 is equal to $^1/_2$ of the H_2 deposition rate. The NPP values of both of these anaerobic ecosystems are far lower than modern marine NPP. Our calculated NPP values for Case 2 range from approximately (1–7) × 10^{12} mol C $year^{-1}$, or approximately 500–3000 times lower than the modern marine value. For Case 3 they range from

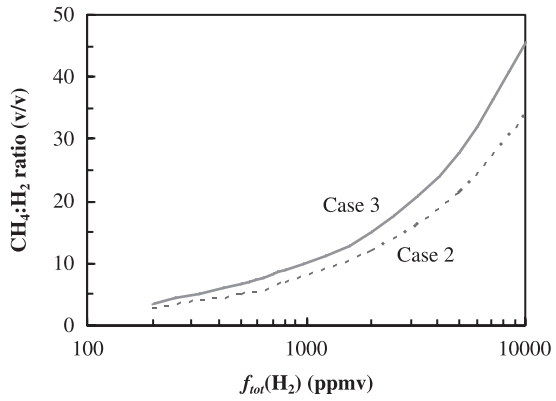

Fig. 10 Calculated CH_4: H_2 ratio as a function of $f_{tot}(H_2)$ for both the Case 2 and the Case 3 ecosystems. The Case 3 values are higher because the phototrophs utilize H_2 more efficiently than the methanogens.

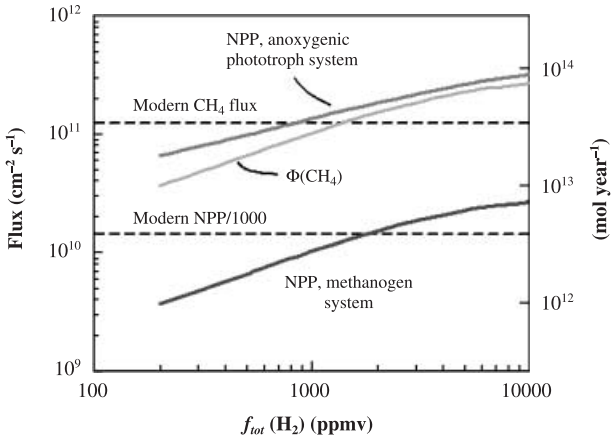

Fig. 11 Global net primary productivity (NPP) and CH_4 flux as a function of $f_{tot}(H_2)$ for Cases 2 and 3. Shown for reference are the modern value of the global CH_4 flux and marine NPP (scaled down by 1000). For Case 2, NPP = $^1/_{10}$ $\Phi(CH_4)$, and for Case 3, NPP = $^1/_2$ $\Phi_{dep}(H_2)$ + $^1/_{10}$ $\Phi(CH_4)$.

approximately (2–9) × 10^{13} mol C $year^{-1}$, or approximately 40–200 times lower than today. As has been pointed out previously by others (e.g. Walker, 1977), primary productivity should have increased dramatically after oxygenic photosynthesis evolved because abundant H_2O could then be used as a reductant (see Discussion section).

The important fluxes in the Case 3 global hydrogen budget are shown in Fig. 12. A CH_2O burial efficiency of 2% has been assumed. The figure illustrates several points. First, nearly all of the outgassed hydrogen in this model is eventually lost by escape to space, as opposed to being used to reduce outgassed CO_2 to organic carbon. The same is true to an even greater extent for Case 2. This result is a consequence of our assumption that hydrogen escapes as rapidly as possible, i.e. at the diffusion limit, and that the organic carbon burial efficiency was relatively low. If hydrogen escaped more slowly than we have assumed, as suggested by Tian *et al.* (2005), then calculated

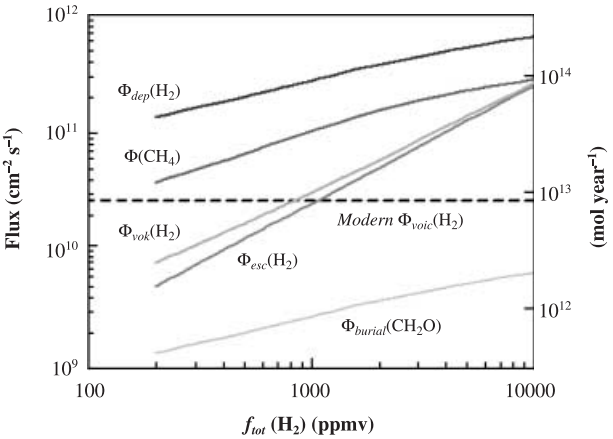

Fig. 12 Hydrogen budget for the Case 3 ecosystem. The five curves correspond to the five terms of the hydrogen budget, as described in the text and Appendix 1. For the case shown here, we assume that 2% of the organic matter produced by the phototrophs is removed through burial in marine sediments (i.e. $\Phi_{burial}(CH_2O)$ = 2% NPP).

$f_{tot}(H_2)$ values would have been correspondingly higher at a given outgassing rate and more of the outgassed hydrogen would have gone into reducing CO_2, leading to correspondingly higher NPP and organic carbon burial fluxes.

Second, the deposition flux of H_2 into the ocean is considerably higher than the volcanic flux of H_2. Because all of the downward-flowing H_2 is assumed to be fueling anoxygenic photosynthesis in this case, this implies that primary productivity is *not* limited by the volcanic outgassing rate. Recycling of hydrogen and methane within the atmosphere–ocean system allows productivity to exceed the supply of reductants from outside the system. This result should not be surprising: the same thing happens to an even greater extent in a closed ecosystem such as a sulphuretum, in which organisms can thrive despite a complete lack of supply of reductants from outside. Note that the recycling is much more effective at low values of $f_{tot}(H_2)$ than it is at higher values. (The ratio $\Phi_{dep}(H_2)$:$\Phi_{volc}(H_2)$ ranges from approximately 25 at low values of $f_{tot}(H_2)$ to approximately 2.5 at high values.) This is because photochemistry is more effective at converting CH_4 back into H_2 when the atmospheric CH_4 concentration is relatively low. At high CH_4 concentrations, short-wavelength UV photons become limiting, so the lifetime of CH_4 increases and the recycling rate is capped. This, in turn, suggests that at high H_2 outgassing rates, biological productivity may be affected by the short-wavelength UV flux from the Sun (see Discussion).

Case 4: Sulphur-based ecosystem

We now turn our attention to an ecosystem based on sulphur metabolism, R7 and R8. As discussed earlier, such an ecosystem may actually have preceded one based on H_2, but then later on it would have operated in tandem with H_2-based metabolism. For consistency with the cases above, we

assumed that the sulphur reducers (R7) have the same 1 : 10 growth yield as the H_2-using methanogens; that is, they consume 10 mol of S per mole of biomass they produce. Thus, their NPP is equal to $^8/_{10}$ of the S_8 deposition flux. (In laboratory studies, e.g. Fischer *et al.*, 1983, the observed growth yield is about half of this value; this would simply serve to decrease our NPP values by $^1/_2$.) We took NPP for the sulphur phototrophs (R8) to be $^1/_2$ of the H_2S deposition flux. Because the SO_2 outgassing rate was likely approximately 10^{11} mol year^{-1} (Ono *et al.*, 2003), and the H_2 outgassing rate was set at approximately 5×10^{12} mol year^{-1}, we expected that this ecosystem would show lower NPP values than our H_2-based ones.

Figure 13 illustrates the NPP values of both microbial groups in this ecosystem as a function of the CH_4:H_2 ratio. As the CH_4:H_2 ratio increases from 0.006 to 0.5, the NPP values for the sulphur-reducing bacteria range from approximately 5.9×10^7–3.7×10^9 mol C year^{-1}. The NPP of the H_2S-using phototrophs is slightly higher, approximately 4.7×10^9–6.7×10^9 mol C year^{-1}. The dependence of NPP of the sulphur reducers on the atmospheric CH_4:H_2 ratio is a consequence of the photochemistry: As the CH_4:H_2 ratio increases, more CO is produced from photo-oxidation of CH_4. This produces more HCO, which in turn creates more HS, which creates more S_2, and ultimately, more S_8. (For the detailed chemistry, see Pavlov & Kasting, 2002.)

The total NPP for our sulphur-based ecosystem is 5–6 orders of magnitude lower than modern marine NPP and 2–4 orders of magnitude lower than for our H_2-based ecosystems (compare Figs 11 and 13). Furthermore, within the sulphur-based system, the NPP of the phototrophs is generally much higher (up to 80 times) than that of the sulphur reducers. Both results, however, should be viewed cautiously, as we have neglected internal recycling of sulphur within the surface ocean ecosystem. Unlike the case of the H_2-based ecosystem, there is no straightforward way of predicting internal recycling rates. For the H_2-based ecosystem, the rate of recycling was governed by atmospheric photochemistry and diffusion rates through the atmosphere–ocean interface. For the sulphur-based ecosystem, the recycling rate would be determined by microbial population dynamics within the surface ocean.

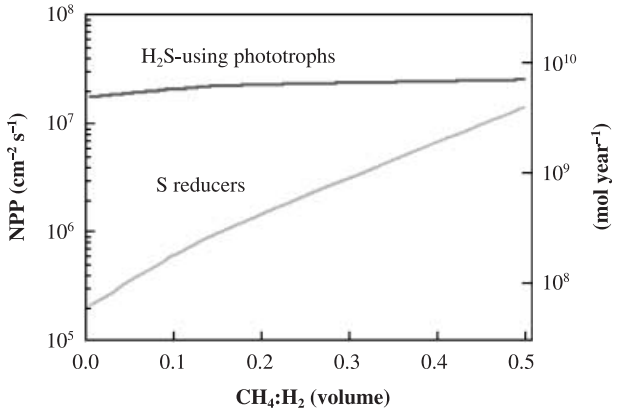

Fig. 13 NPP of H_2S-using phototrophs and S-reducing bacteria, plotted as a function of atmospheric CH_4:H_2 ratio for $f_{tot}(H_2)$ = 800 ppmv. The chemistry that affects the S reducers is described in the text.

It is instructive to compare these results to those obtained by Canfield (2005). Canfield's sulphur-based ecosystem model was more sophisticated in the sense that it did incorporate biotic nutrient recycling. Canfield assumed that H_2S-using phototrophs in Archean microbial mats could have oxidized hydrothermally derived sulphide to sulphate, much of which would then have been reduced back to sulphide by bacterial sulphate reduction. In turn, this secondary sulphide could have further fuelled the phototrophs, thereby completing the recycling loop. Using this approach, Canfield (2005) obtained NPP values ranging from $(2–20) \times 10^{13}$ mol C year^{-1}. These values are approximately 3–4 orders of magnitude higher than our sulphur-based NPP values and are therefore comparable to the NPP of our H_2-based ecosystems (see Table 2). We do not, however, consider these high rates of sulphur metabolism to be plausible. Canfield's model assumes that essentially all of the sulphide emitted by mid-ocean ridge hydrothermal vents reaches the surface ocean. In reality, if the deep oceans were rich in ferrous iron, most of this hydrothermal sulphide should have reacted with dissolved Fe^{2+} to form pyrite (Walker & Brimblecombe, 1985). Only the sulphur emitted from surface volcanism would have been available to surface organisms. Thus, perhaps a realistic estimate for sulphur-based NPP probably lies somewhere between Canfield's value and ours. If we multiply our S-based NPP values by a factor of 10 (Canfield's assumed recycling efficiency), our estimated maximum rate of S-based NPP is approximately 10^{11} mol C year^{-1}, which is still a factor of 100–1000 times smaller than our H_2-based NPP values.

Case 5: Iron-based ecosystem

Deriving limits on iron-based metabolism requires a different approach, as iron would not have entered the early oceans primarily through the atmosphere. (Paradoxically, iron *does* enter the oceans from the atmosphere today, as dust; however, much larger sources of iron were available to the reduced early oceans.) We can derive plausible constraints on the productivity of Fe^{2+}-oxidizing phototrophs as follows: The concentration of dissolved Fe^{2+} in the Archean deep oceans, a_{Fe}, is estimated to have been approximately 3 ppm by weight or 0.054 mol m^{-3} (Holland, 1984; p. 388). This estimate is based partly on the relative solubilities of siderite and calcite, and partly on the amount of iron needed to form banded iron-formations. This Fe-rich water would have been brought to the surface in upwelling zones, as deep water is today. The rate at which deep water is upwelled globally today can be estimated by dividing the average depth of the oceans, 4 km, by the deep ocean turnover time, approximately 1000 year (Broecker & Peng, 1982). This yields an upwelling rate, v_{up}, of 4 m year^{-1} or 0.01 m day^{-1}. The area of Earth's surface is 5.1×10^{14} m^2,

and oceans cover approximately 70% of this area, so the area covered by oceans, A_o, is 3.6×10^{14} m^2. We assume that the growth yield, g, of Fe^{2+}-oxidizing phototrophs is 0.25 mol C mol^{-1} Fe^{2+}. Thus, assuming that all of this upwelled iron was used by the Fe^{2+}-oxidizing phototrophs, the average NPP of Fe^{2+}-oxidizing phototrophs would have been $v_{up} \cdot a_{Fe} \cdot A_o \cdot g = 1.9 \times 10^{13}$ mol C year^{-1}.

Recall that our most productive H_2-based ecosystem yields rates of $(2–9) \times 10^{13}$ mol C year^{-1}. Hence, our model predicts that iron-based NPP was slightly lower than H_2-based NPP. By comparison, Canfield (2005) obtained Fe^{2+}-based NPP values of approximately $(2–6) \times 10^{14}$ mol C year^{-1}, which are 10–30 times higher than our estimate. His approach was based on the stoichiometry of Fe^{2+}-oxidizing photosynthesis and an assumed Redfield ratio equal to the modern marine value. We would argue that our estimate is therefore more plausible because Canfield assumes that Archean productivity scaled to modern productivity (i.e. it was P-limited), whereas we do not.

Such global average numbers are misleading, in a sense, because upwelling regions are localized in certain coastal zones and near the equator (Kump *et al.*, 2004). In the open ocean, the maximum upwelling rate is approximately 0.2 m day^{-1}, whereas in coastal regions it may range as high as 1 m day^{-1} (Broecker & Peng, 1982). The latter value is approximately 100 times higher than the average upwelling rate, so productivity in such regions could also be 100 times higher than just calculated. Thus, the local NPP for iron-reducers in coastal zones could have been of order 0.04 mol m^{-2} day^{-1}, or 2×10^{13} cm^{-2} s^{-1}. This is about half the modern NPP value in upwelling regions, which is approximately 1 g C m^{-2} day^{-1}, or 0.083 mol m^{-2} day^{-1} (Riley & Chester, 1971, p. 264; see also Kasting, 1992). However, these NPP values are so high that phosphate may have become limiting. If Bjerrum & Canfield (2002) are correct, and phosphate levels were only 10–25% of present levels, then the rate of Fe-based metabolism would be reduced by a factor of 2–5. Recall that H_2-based metabolism rates may also have been reduced by a similar amount as a consequence of P limitation. Hence, estimated global rates of H_2- and Fe-based metabolism remain roughly the same.

Spatially, then, the Archean marine ecosystem would have been subdivided into different regions based on nutrient kinetics and relative biological productivity. In upwelling regions, iron would have titrated out all the sulphur, and Fe-based metabolism would have dominated. Elsewhere, sulphur deposited from the atmosphere would likely have titrated out the iron. H_2-based metabolism could have proceeded everywhere and may well have dominated over much of the ocean.

DISCUSSION

H_2 escape rates and implications for Archean climate

An explicit assumption in all of our coupled model calculations is that H_2 escape to space was limited by molecular diffusion through the homopause (100 km), as it is today, so that the H_2 escape flux was given by Eqn 3. This may not necessarily have been true. Unlike the hot modern exosphere, the Archean exosphere was probably cold due to the paucity of O_2 (a good UV absorber) and the relatively high level of CO_2 (a good IR emitter). Thus, energy limitations may have reduced the escape rate, especially at higher values of $f_{tot}(H_2)$. This could ultimately have resulted in $f_{tot}(H_2)$ values and corresponding CH_4 mixing ratios even higher than presented here. The recent paper by Tian *et al.* (2005) supports the idea that hydrogen escape was much slower than the diffusion limit. We note, however, that they considered only hydrodynamic escape, whereas in reality other nonthermal hydrogen escape mechanisms may have been important, as shown by Kumar *et al.* (1983) for early Venus. Thus, the actual escape rate may have been intermediate between the values that they calculate and the much faster escape rates assumed here.

If Tian *et al.* are at least partly correct and the hydrogen escape rate was indeed far lower (approximately 100 times) than our assumed rate, then our model makes some interesting predictions for climatic and biological evolution. Taken together, Eqns 2 and 3 imply that for a given hydrogen outgassing rate, $f_{tot}(H_2)$ would be higher in a methanogen-dominated ecosystem (Case 2) than in a phototroph-dominated ecosystem (Case 3), because methanogens are much less productive than phototrophs. Thus, much less organic matter would be buried in a methanogen-dominated system, and so the atmosphere–ocean H_2 balance (Eqn 2) would essentially have been between volcanic outgassing and escape to space only. If methanogens evolved before anoxygenic phototrophs, as phylogenetic evidence suggests (Battistuzzi *et al.*, 2004), this implies that $f_{tot}(H_2)$ could have been very high, around 0.07. Methanogens should have converted most of the H_2 into CH_4 (Fig. 10), so CH_4 concentrations could have approached 0.07÷2 = 3.5%. This is higher than the range of values that has been studied with climate models. Pavlov *et al.* (2000) showed that a CH_4 concentration of 1% could produce approximately 50 degrees of greenhouse warming. Depending on how much CO_2 was also present, surface temperatures could conceivably have been as high as the 55–85 °C estimated from oxygen isotopes in 3.3-Ga Barberton cherts (Knauth & Lowe, 2003). We have not attempted to calculate the greenhouse effect of these higher CH_4 concentrations because we have learned that the Pavlov *et al.*, 2000) climate model does a poor job of calculating absorption of incoming solar near-IR radiation in the stratosphere. This problem is currently being addressed. It seems plausible, though, that an early Archean Earth with a methanogen-based ecosystem could have been very warm.

This scenario is consistent with the oft-noted observation that most of the organisms located at the base of the r-RNA phylogenetic 'tree of life' are thermophilic (Woese, 1987). In our model, this could be explained by a globally hot climate

that developed after methanogens evolved, perhaps around 3.8 Ga (Battistuzzi *et al.*, 2004). All organisms living at this time would have experienced this climate, including the sulphur metabolizers that may have evolved earlier, and so all of them should exhibit this same trait. Other possible explanations for basal thermophily include a hot origin for life itself or resetting of temperature tolerances as a consequence of large impacts (Gogarten-Boekels *et al.*, 1995).

According to Tice & Lowe (2004), anoxygenic phototrophs appear to have evolved by approximately 3.4 Ga. Their analysis is based on observations of the Buck Reef chert in South Africa. Molecular clock analysis yields a roughly comparable date for this event, approximately 3.2 Ga (Battistuzzi *et al.*, 2004). So, anoxygenic photosynthesis probably became a dominant mode of primary productivity by the early Archean. Once this had happened, the rate of organic carbon burial should have increased by roughly a factor of 10 (representing the difference in NPP between Case 2 and Case 3 – see Fig. 11). At this time, both $f_{tot}(H_2)$ and atmospheric CH_4 levels should have decreased. If organic carbon burial follows the roughly logarithmic trend seen in Figs 11 and 12, then $f_{tot}(H_2) \approx 2\%$ for Case 3, which implies that $f(CH_4) \approx 1\%$. A climate calculation would be needed to determine by how much the Archean climate should have cooled. After *oxygenic* photosynthesis evolved, probably sometime before 2.7 Ga (Brocks *et al.*, 1999; Summons *et al.*, 1999), CH_4 levels would have increased a second time (see below) and the climate may have warmed once again. By approximately 2.3 Ga, however, free O_2 began to accumulate in the atmosphere, destroying the methane greenhouse and perhaps triggering the Palaeoproterozoic glaciations, as suggested by previous authors (Pavlov *et al.*, 2000).

The upper limit on CH_4 might also have been influenced by processes other than those considered here. As discussed by Zahnle (1986) and Pavlov *et al.* (2001a), atmospheric CH_4:CO_2 ratios exceeding unity would have led to the formation of hydrocarbon haze, as occurs today on Saturn's moon Titan. This haze should have caused an 'antigreenhouse' effect (McKay *et al.*, 1991) that would have cooled the surface by absorbing solar radiation in the upper atmosphere and emitting it back to space. Ultimately, if the mean surface temperature fell below freezing, the ocean would have frozen over and CH_4 production would have ceased almost entirely. Hence, if hydrogen escape was indeed slow, the CH_4 concentration may actually have been determined by the atmospheric CO_2 level. The CH_4 abundance could have been as high as that of CO_2, but not higher, because that is when organic haze would have formed. The CO_2 concentration itself is hard to estimate from first principles because it depends on a variety of poorly constrained factors, such as continental size, outgassing rates, and the efficiency of seafloor weathering (Sleep & Zahnle, 2001). A detailed understanding of Archean palaeoclimate must rely on better knowledge of the geological record.

Effects of solar UV radiation on ecosystem productivity

Astronomical observations show that young solar-type stars emit significantly more UV radiation than does the Sun (Canuto *et al.*, 1982, 1983; Zahnle & Walker, 1982; Walter & Berry, 1991; Guinan & Ribas, 2002). This suggests that during the Archean, the solar UV flux should have been several times higher than the modern flux that we have assumed in all of our calculations. As mentioned earlier, for higher levels of $f_{tot}(H_2)$ photochemical conversion of CH_4 into H_2 would have been limited by the solar UV flux, most notably by the availability of Lyman-α photons (λ = 121.6 nm). This photochemistry, combined with atmospheric oxidation of CH_4 to eventually form CO_2, constitutes the abiotic reverse of R1 (which is biotic). Thus, we would expect that if we increase the solar far-UV flux in our model, both the CH_4 flux and the primary productivity should increase significantly in the higher $f_{tot}(H_2)$ regimes.

To test this hypothesis, we conducted sensitivity tests using our coupled model for both high and low values of $f_{tot}(H_2)$. (For convenience, we actually fixed $f(CH_4)$ rather than $f_{tot}(H_2)$. This must be borne in mind when analysing the results.) We repeated our simulations for our Case 3 ecosystem using two different perturbations: one in which we increased the solar Lyman-α flux by a factor of 2.5, and one in which we increased the entire solar far-UV flux using a wavelength-dependent scaling factor of $10^{\left(\frac{200-\lambda}{200}\right)}$ (Pavlov *et al.*, 2001a), with λ in nm. The results of these analyses are shown in Table 3. As expected, for all increased-UV simulations we calculated significant (25–80%) increases in H_2 and CO deposition, as well as in CH_4 production and primary productivity. Likewise, the H_2 and CO surface mixing ratios also increased significantly in all of the sensitivity runs. (Had we performed these calculations at fixed $f_{tot}(H_2)$, CH_4 would have decreased slightly to compensate for the H_2 increase; however, the increases in CH_4 flux and productivity would have been nearly the same.) All of these increases were much larger for high $f_{tot}(H_2)$ values than for low ones, consistent with the greater demand for photons in these cases. Thus, ecosystem productivity during the early Archean may have been partly controlled by the solar far-UV flux.

Constraints imposed by the carbon isotope record

One way of testing the validity of these results is to compare the predictions of the model with the carbon isotope record in rocks. An observation that has stood the test of time fairly well (Schidlowski *et al.*, 1983; DesMarais *et al.*, 1992; DesMarais, 1997; Kump *et al.*, 2001) is that the $\delta^{13}C$ values of carbonate rocks have remained close to 0‰ throughout most of geological time. (Some remarkable, short-lived excursions in $\delta^{13}C$ have occurred, e.g. at 2.0–2.2 Ga [Karhu & Holland, 1996], but these are not pertinent to the discussion here.) The $\delta^{13}C$ values of organic carbon (kerogen) in rocks are more scattered,

Table 3 Results of solar UV sensitivity analyses for Case 3*

Original values								
$f_{tot}(H_2)$	$f(CH_4)$	$f(H_2)$	$f(CO)$	$\Phi_{dep}(H_2)$	$\Phi_{dep}(CO)$	$\Phi(CH_4)$	NPP†	NPP‡
800	372	42	35.9	2.45×10^{11}	1.07×10^{11}	8.93×10^{10}	1.31×10^{11}	3.50×10^{13}
10000	4927	108	171	6.45×10^{11}	5.09×10^{11}	2.80×10^{11}	3.51×10^{11}	9.38×10^{13}
Changes after increasing Lyman–α flux								
$f_{tot}(H_2)$	$f(CH_4)$	$f(H_2)$	$f(CO)$	$\Phi_{dep}(H_2)$	$\Phi_{dep}(CO)$	$\Phi(CH_4)$	NPP†	NPP‡
800	372	50.7	49	3.02×10^{11}	1.46×10^{11}	1.12×10^{11}	1.62×10^{11}	4.34×10^{13}
10000	4927	161	270	9.57×10^{11}	8.04×10^{11}	4.54×10^{11}	5.24×10^{11}	1.40×10^{14}
Changes after increasing far UV								
$f_{tot}(H_2)$	$f(CH_4)$	$f(H_2)$	$f(CO)$	$\Phi_{dep}(H_2)$	$\Phi_{dep}(CO)$	$\Phi(CH_4)$	NPP†	NPP‡
800	372	50.5	48.7	3.00×10^{11}	1.45×10^{11}	1.11×10^{11}	1.61×10^{11}	4.01×10^{13}
10000	4927	173	306	1.03×10^{12}	9.12×10^{11}	4.83×10^{11}	5.63×10^{11}	1.51×10^{14}

*All fluxes are given in units of molecules cm^{-2} s^{-1}, and mixing ratios are ppm by volume.
†NPP in molecules C cm^{-2} s^{-1}, where NPP = $^1/_2$ $\Phi_{dep}(H_2)$ + $^1/_{10}$ $\Phi(CH_4)$.
‡NPP in mol C $year^{-1}$, where 1 mol $year^{-1}$= 0.00374 molecules cm^{-2} s^{-1}.

but most values fall in the range of –20‰ to –40‰, with an average near –25‰ (Schidlowski *et al.*, 1983; Pavlov *et al.*, 2001b). In the conventional interpretation of the C isotope record, mass-balance arguments can be used to show that the fraction of outgassed CO_2 buried as organic carbon, f, is given by:

$$f = \frac{\delta_{carb} - \delta_{in}}{\Delta_B} \quad (7)$$

Here, δ_{carb} is the $\delta^{13}C$ value of carbonates, δ_{in} is the $\delta^{13}C$ value of mantle carbon (–5‰), and Δ_B is the fractionation between carbonates and organic carbon (25‰ in this case). Hence, according to this conventional viewpoint, δ_{carb} values near 0‰ throughout most of geological time imply that f has remained near 20%. A perceived increase in Δ_B going back in time through the Proterozoic may imply that f was only approximately 10% during the Archean (DesMarais *et al.*, 1992). The value of f during the Archean may have been even smaller if the recent reinterpretation of the carbon isotope record by Bjerrum & Canfield (2004) is correct (see below).

Holland (1984, 2002) has attempted to explain the apparent near-constancy of f by arguing that it was controlled by the relative rates of supply of volcanic H_2 and CO_2. He assumed that outgassed H_2 was used to reduce some of the outgassed CO_2 to organic carbon by the reaction:

$$CO_2 + 2\ H_2 \rightarrow CH_2O + H_2O. \quad (R10)$$

According to Holland (2002), the present volcanic H_2 flux is 5×10^{12} mol $year^{-1}$, or 1.9×10^{10} cm^{-2} s^{-1}, while the outgassed CO_2 flux is 6×10^{12} mol $year^{-1}$, or 2.2×10^{10} cm^{-2} s^{-1}. Holland argued that if all of the outgassed H_2 was used to reduce CO_2, then 42% of the outgassed CO_2 could be buried as organic carbon. Roughly half the H_2 is used to reduce SO_2 to pyrite (FeS_2) in Holland's model, though, yielding an f value of approximately 20%, as required by the carbon isotope data. In full detail, the argument is more complicated than presented here, as carbon also enters the atmosphere–ocean system from weathering of carbonate rocks and kerogens on land. If one assumes that the reservoirs of continental carbonates and kerogen are in steady state, though, then the numbers reduce to those given here. This is nothing more than the requirement for global redox balance applied to the modern, oxygenic Earth system.

Our model makes predictions about the organic carbon burial rate that can be tested against the carbon isotope record if one assumes that Holland's estimate of the molar ratio of outgassed CO_2 to H_2 (6 : 5) is correct. Organic carbon burial fluxes are given in Fig. 12 as a function of $f_{tot}(H_2)$. As mentioned earlier, they are 13–20 times higher for Case 3 than for Case 2 because the anoxygenic phototrophs synthesize much more organic carbon per unit of CH_4 produced. A quick look at the numbers shows that in the methanogen-based ecosystem (Case 2), organic carbon burial never accounts for more than about 0.3% of outgassed CO_2, in complete disagreement with the carbon isotope record. Three different reasons for this discrepancy can be imagined: (1) the escape rate of hydrogen to space is overestimated in the model; (2) the burial efficiency of organic carbon is underestimated; or (3) methanogens have never dominated primary productivity during the time period since about 3.2 Ga when a reasonably good carbon isotope record exists. Given a presumed early origin for anoxygenic phototrophs, along with their ability to outcompete methanogens at low H_2 levels, explanation (3) seems entirely reasonable. However, the Tian *et al.* (2005) result shows that explanation (1) may also be relevant.

In contrast, our Case 3 ecosystem is consistent with the conventional view of the carbon isotope record in some, but not all, cases. It is instructive to look at these numbers in somewhat more detail. Holland's estimated present day volcanic H_2 flux supports a total hydrogen mixing ratio of just under 800 ppmv in our model. The exact concentration depends on the organic carbon burial efficiency, which has been assumed to range between 0.2% and 2%. Consider the case in which

$f_{tot}(H_2)$ = 200 ppmv (our lowest outgassing case) and the organic carbon burial efficiency is 2%. The calculated H_2 outgassing rate for this simulation is 2.1×10^{12} mol year^{-1}, so the corresponding volcanic CO_2 flux should be $^6/_5$ that value, or 2.5×10^{12} mol year^{-1}. The calculated burial flux of organic carbon for this case is 3.7×10^{11} mol year^{-1}. Thus, the ratio of buried organic carbon to outgassed CO_2 is 0.15. This is in fairly good agreement with the value of 0.2 predicted from carbon isotopes, indicating that our model yields reasonable results at low volcanic outgassing rates.

The same is not true, though, at high outgassing rates. Figure 12 shows that while $\Phi_{volc}(H_2)$ scales linearly with $f_{tot}(H_2)$, the organic carbon burial rate does not. Proportionately less internal recycling of H_2 and CH_4 occurs at high values of $f_{tot}(H_2)$, and more of the outgassed H_2 escapes to space. The result is that, at $f_{tot}(H_2)$ = 10 000 ppmv, the calculated ratio of buried organic carbon to outgassed CO_2 is only approximately 0.02 – about 1/10th the value inferred from carbon isotopes. These higher values of $f_{tot}(H_2)$ are expected for a hot, volcanically active young Earth; hence, our model underpredicts the organic carbon burial rate for the most realistic simulations. The most likely explanation is that Tian *et al.* (2005) are correct, and hydrogen escaped to space at a rate much slower than the diffusion limit. Slow hydrogen escape is thus consistent both with the carbon isotope record and with Holland's early proposals for what limits organic carbon burial.

The carbon burial rate as represented in our methanogenic ecosystems (Cases 1 and 2) assumes that methanogen growth is essentially continuous and always keeps up with metabolism – that is, the ratio of carbon assimilation to metabolism is fixed. In reality, this may not be true. Once the methanogen population has reached steady state, the assimilation to metabolism ratio may decline. This would make Cases 1 and 2 even less consistent with the conventional view of the C isotope record.

Thus far, our discussion has been predicated on the conventional interpretation of the carbon isotope record. Recently, Bjerrum & Canfield (2004) suggested that hydrothermal alteration (carbonatization) of ocean crust should be included in the mass balance that leads to Eqn 7. If the carbon isotopic composition of the deep ocean was different from that of the surface ocean, as today – the modern deep ocean is enriched in ^{12}C relative to ^{13}C – then Eqn 7 would have to be modified. That analysis suggests that the value of f was between 0 and 10% throughout the Archean. Such a result is consistent with virtually all of our anaerobic ecosystem models.

However, Nakamura & Kato (2004) have recently measured the $\delta^{13}C$ values of carbonates in 3.5-Ga carbonatized ocean basalts and found them to be -0.3 ± 1.2‰, suggesting that the gradient in carbon isotope composition between the surface and deep ocean was small at that time. This agrees with what one might expect theoretically: the biological pumping of particulate organic carbon into the deep ocean should have been less efficient during the Archean than it is today due to the absence of zooplankton and faecal pellets. Hence, we believe that the conventional interpretation of the carbon isotope record is essentially correct. This, in turn, implies that hydrogen escape must have been relatively slow in order to allow sufficient organic carbon to be buried.

Changes induced by the advent of oxygenic photosynthesis

For completeness, we discuss briefly the changes in NPP and methane production that should have resulted following the origin of oxygenic photosynthesis. In such a biosphere, the limitations imposed by availability of reductants would have been overcome and productivity *should* have been limited by the supply of phosphorus. NPP could have risen to essentially modern values, subject to constraints on P availability as discussed by Bjerrum & Canfield (2004). As discussed by other authors (Catling *et al.*, 2001), CH_4 production should have risen as a consequence of the increased production of organic matter and a corresponding increase in rates of fermentation and methanogenesis in sediments (R4 and R5). As in the ensuing Proterozoic Eon, recycling of organic matter by aerobic decay and sulphate reduction would have been inefficient (Canfield, 2005). CH_4 fluxes from marine sediments could therefore have been as high as 10–20 times the modern (mostly terrestrial) biogenic flux (Pavlov *et al.*, 2003), although this prediction depends on the uncertain rate of consumption by methanotrophs living in consortium with sulphate reducers in sediments (Hinrichs *et al.*, 1999). We nonetheless concur with the conclusion of Catling *et al.* (2001): atmospheric CH_4 concentrations should have increased following this event, causing the climate to warm and possibly increasing the rate of hydrogen escape to space. An advent of oxygenic photosynthesis around 2.7 Ga (Brocks *et al.*, 1999; Summons *et al.*, 1999) could have resulted in a warm Late Archean.

CONCLUSIONS

A coupled photochemical-ecosystem model has been developed to estimate CH_4 production and net primary productivity in the anaerobic Archean marine biosphere, before the origin of oxygenic photosynthesis. CH_4 fluxes predicted by the completely anaerobic model are within a factor of 3 of the modern biogenic CH_4 flux over a wide range of parameter values. This suggests that atmospheric CH_4 concentrations should have risen to at least approximately 1000 ppmv soon after methanogens evolved. Hence, CH_4 could have had an important effect on climate since the early Archean, or whenever life itself originated on Earth.

H_2-based metabolism was probably slightly more productive than ferrous iron-based metabolism on a global basis, but the latter should have dominated marine productivity in upwelling zones. Sulphur-using organisms were likely present in nonupwelling regions of the Archean surface ocean. Their productivity in our model is low; however, in reality, recycling

of sulphur within the surface ocean might have allowed sulphur metabolism to proceed rapidly as well. Further studies are needed to examine this question.

If H_2-using methanogens evolved before anoxygenic phototrophs (which appears likely), and if hydrogen escape rates were slow, our results suggest that the Archean Earth might have experienced a relatively hot period (with significant greenhouse warming by CH_4), followed by a cooler period after phototrophs arose. This is because a phototroph-dominated ecosystem would have been much more productive than a methanogen-dominated one, and would therefore have a lower $f_{tot}(H_2)$ value, and thus, less CH_4 to warm the climate. The advent of oxygenic photosynthesis would have led to a second increase in atmospheric CH_4 and a warm Late Archean climate. This warm period ended with the rise of atmospheric O_2 at approximately 2.3 Ga, which may have triggered the Palaeoproterozoic glaciations.

Some or most of our ecosystem scenarios are consistent with the carbon isotope record, depending on whether one accepts the conventional interpretation of the record or the alternative interpretation of Bjerrum & Canfield (2004). We favour the conventional interpretation for reasons discussed earlier. An ecosystem based on anoxygenic photosynthesis, coupled with slow escape of hydrogen to space, could have produced sufficient organic carbon burial to match this interpretation. More evidence from the geological and biological records is needed to test the predictions of this fairly complex ecological model.

ACKNOWLEDGEMENTS

Funding for this work was provided by the NASA Exobiology and NSF LExEn programs. We thank our Penn State colleagues Lee Kump, Blair Hedges, and Chris House for their valuable feedback.

REFERENCES

Arthur MA, Dean WE, Neff ED, Hay BJ, King J, Jones G (1994) Varve-calibrated records of carbonate and organic carbon accumulation over the last 2000 years in the Black Sea. *Global Biogeochemical Cycles* **8**, 195–217.

Battistuzzi FB, Feijão A, Hedges SB (2004) A genomic timescale of prokaryote evolution: insights into the origin of methanogenesis, phototrophy, and the colonization of land. *BMC Evolutionary Biology* **4**, 44–57.

Berner RA (1982) Burial of organic carbon and pyrite sulfur in the modern ocean – its geochemical and environmental significance. *American Journal of Science* **282**, 451–473.

Bjerrum CJ, Canfield DE (2002) Ocean productivity before about 1.9 Gyr ago limited by phosphorus adsorption onto iron oxides. *Nature* **417**, 159–162.

Bjerrum CJ, Canfield DE (2004) New insights into the burial history of organic carbon on the early Earth. *Geochemistry, Geophysics and Geosystems* **5**, 2004GC000713.

Brocks JJ, Logan GA, Buick R, Summons RE (1999) Archean molecular fossils and the early rise of eukaryotes. *Science* **285**, 1033–1036.

Broda E, Peschek GA (1983) Nitrogen fixation: evidence for the reducing nature of the early biosphere. *Biosystems* **16**, 1–8.

Broecker WS, Peng TH (1982) *Tracers in the Sea*. Lamont-Doherty Geological Observatory, New York.

Canfield DE (1998) A new model for Proterozoic ocean chemistry. *Nature* **396**, 450–453.

Canfield DE (2005) The early history of atmospheric oxygen: homage to Robert M. Garrels. *Annual Review of Earth and Planetary Sciences* **33**, 1–36.

Canfield DE, Habicht KS, Thamdrup B (2000) The Archean sulfur cycle and the early history of atmospheric oxygen. *Science* **288**, 658–661.

Canuto VM, Levine J, Augustsson T, Imhoff C (1982) UV radiation from the young Sun and oxygen levels in the pre-biological paleoatmosphere. *Nature* **296**, 816–820.

Canuto VM, Levine JS, Augustsson TT, Imhoff CL, Giampapa MS (1983) The young Sun and the atmosphere and photochemistry of the early Earth. *Nature* **305**, 281–286.

Catling DC, Zahnle KJ, McKay CP (2001) Biogenic methane, hydrogen escape, and the irreversible oxidation of early Earth. *Science* **293**, 839–843.

Cloud P (1976) Beginnings of biospheric evolution and their biogeochemical consequences. *Paleobiology* **2**, 351–387.

Conrad R (1999) Contribution of hydrogen to methane production and control of hydrogen concentrations in methanogenic soils and sediments. *FEMS Microbiology Ecology* **28**, 193–202.

Daniels L, Fuchs G, Thauer RK, Zeikus JG (1977) Carbon monoxide oxidation by methanogenic bacteria. *Journal of Bacteriology* **132**, 118–126.

DesMarais DJ (1997) Isotopic evolution of the biogeochemical carbon cycle during the Proterozoic Eon. *Organic Geochemistry* **27**, 185–193.

DesMarais DJ (1998) Earth's early biosphere. *Gravitational and Space Biology Bulletin* **11**, 23–30.

DesMarais DJ, Strauss H, Summons RE, Hayes JM (1992) Carbon isotope evidence for the stepwise oxidation of the Proterozoic environment. *Nature* **359**, 605–609.

Ehrenreich A, Widdel F (1994) Anaerobic oxidation of ferrous iron by purple bacteria, a new type of phototrophic metabolism. *Applied and Environmental Microbiology* **60**, 4517–4526.

Fardeau ML, Belaich JP (1986) Energetics of the growth of *Methanococcus thermolithotrophicus*. *Archives of Microbiology* **144**, 381–385.

Fay P (1992) Oxygen relations of nitrogen fixation in cyanobacteria. *Microbiological Reviews* **56**, 340–373.

Fischer F, Zillig W, Stetter KO, Schreiber G (1983) Chemolithoautotrophic metabolism of anaerobic extremely thermophilic archaebacteria. *Nature* **301**, 511–513.

Genthner B, Bryant M (1982) Growth of *Eubacterium limosum* with carbon monoxide as the energy source. *Applied and Environmental Microbiology* **43**, 70–74.

Gogarten-Boekels M, Hilario E, Gogarten JP (1995) The effects of heavy meteorite bombardment on the early evolution – the emergence of the three domains of life. *Origins of Life and Evolution of the Biosphere* **25**, 251–264.

Gough DO (1981) Solar interior structure and luminosity variations. *Solar Physics* **74**, 21–34.

Guinan EF, Ribas I (2002) Our changing Sun: the role of solar nuclear evolution and magnetic activity on Earth's atmosphere and climate. In *The Evolving Sun and its Influence on Planetary Environments* (eds Montesinos B, Gimenez A, Guinan EF). Astronomical Society of the Pacific, San Francisco, pp. 85–106.

Hayes JM (1983) Geochemical evidence bearing on the origin of aerobiosis, a speculative hypothesis. In *Earth's Earliest Biosphere: its*

Origin and Evolution (ed. Schopf JW). Princeton University Press, Princeton, pp. 291–301.
Hinrichs K-U, Hayes JM, Sylva SP, Brewer PG, DeLong EF (1999) Methane-consuming archaebacteria in marine sediments. *Nature* **398**, 802–805.
Holland HD (1984) *The Chemical Evolution of the Atmosphere and Oceans* Princeton University Press, Princeton, NJ.
Holland HD (2002) Volcanic gases, black smokers, and the Great Oxidation Event. *Geochimica et Cosmochimica Acta* **66**, 3811–3826.
House CH, Runnegar B, Fitz-Gibbon ST (2003) Geobiological analysis using whole genome-based tree building applied to the Bacteria, Archea, and Eukarya. *Geobiology* **1**, 15–26.
Hunten DM (1973) The escape of light gases from planetary atmospheres. *Journal of Atmospheric Science* **30**, 1481–1494.
Huston DL, Logan GA (2004) Barite, BIFs, and bugs: evidence for the evolution of the Earth's early hydrosphere. *Earth and Planetary Science Letters* **220**, 41–55.
Kappler A, Newman DK (2004) Formation of Fe(III)-minerals by Fe(II)-oxidizing photoautotrophic bacteria. *Geochimica et Cosmochimica Acta* **68**, 1217–1226.
Karhu JA, Holland HD (1996) Carbon isotopes and the rise of atmospheric oxygen. *Geology* **24**, 867–870.
Kasting JF (1990) Bolide impacts and the oxidation state of carbon in the Earth's early atmosphere. *Origins of Life* **20**, 199–231.
Kasting JF (1992) Models relating to Proterozoic atmospheric and ocean chemistry. In *The Proterozoic Biosphere: A Multidisciplinary Study* (eds Schopf JW, Klein C). Cambridge University Press, Cambridge, pp. 1185–1187.
Kasting JF, Ackerman TP (1986) Climatic consequences of very high CO_2 levels in Earth's early atmosphere. *Science* **234**, 1383–1385.
Kasting JF, Brown LL (1998) Setting the stage: the early atmosphere as a source of biogenic compounds. In *The Molecular Origins of Life: Assembling the Pieces of the Puzzle* (ed. Brack A). Cambridge University Press, pp. 35–56.
Kasting JF, Catling DC (2003) Evolution of a habitable planet. *Annual Reviews in Astronomy and Astrophysics* **41**, 429–463.
Kasting JF, Pavlov AA, Siefert JL (2001) A coupled ecosystem–climate model for predicting the methane concentration in the Archean atmosphere. *Origins of Life and Evolution of the Biosphere* **31**, 271–285.
Kasting JF, Zahnle KJ, Walker JC (1983) Photochemistry of methane in the Earth's early atmosphere. *Precambrian Research* **20**, 121–148.
Kelley DS, Karson JA, Blackman DK, Fruh-Green GL, Butterfield DA, Lilley MD, Olson EJ, Schrenk MO, Roe KK, Lebon GT, Rivizzigno P (2001) An off-axis hydrothermal vent field near the Mid-Atlantic Ridge at 30°N. *Nature* **412**, 145–149.
Kelley DS, Karson JA, Fruh-Green GL, Yoerger DR, Shank TM, Butterfield DA, Hayes JM, Schrenk MO, Olson EJ, Proskurowski G, Jakuba M, Bradley A, Larson B, Ludwig K, Glickson D, Buckman K, Bradley AS, Brazelton WJ, Roe K, Elend MJ, Delacour A, Bernasconi SM, Lilley MD, Baross JA, Summons RT, Sylva SP (2005) A serpentinite-hosted ecosystem: the Lost City hydrothermal vent field. *Science* **307**, 1428–1434.
Kerby R, Niemczura W, Zeikus J (1983) Single-carbon catabolism in acetogens: analysis of carbon flow in *Acetobacterium woodii* and *Butyribacterium methylotrophicum* by fermentation and ^{13}C nuclear magnetic resonance measurement. *Journal of Bacteriology* **155**, 1208–1218.
Kerby R, Zeikus J (1983) Growth of *Clostridium thermoaceticum* on H_2/CO_2 or CO as energy source. *Current Microbiology* **8**, 27–30.
Kiehl JT, Dickinson RE (1987) A study of the radiative effects of enhanced atmospheric CO_2 and CH_4 on early Earth surface temperatures. *Journal of Geophysical Research* **92**, 2991–2998.
Knauth LP, Lowe DR (2003) High Archean climatic temperature inferred from oxygen isotope geochemistry of cherts in the 3.5 Ga Swaziland Supergroup, South Africa. *GSA Bulletin* **115**, 566–580.
Konhauser KO, Hamade T, Raiswell R, Morris RC, Ferris FG, Southam G, Canfield DE (2002) Could bacteria have formed the Precambrian banded iron formations? *Geology* **30**, 1079–1082.
Kral TA, Brink KM, Miller SL, McKay CP (1998) Hydrogen consumption by methanogens on the early Earth. *Origins of Life and Evolution of the Biosphere* **28**, 311–319.
Kumar S, Hunten DM, Pollack JB (1983) Nonthermal escape of hydrogen and deuterium from Venus and implications for loss of water. *Icarus* **55**, 369–389.
Kump LR, Kasting JF, Barley ME (2001) The rise of atmospheric oxygen and the 'upside-down' Archean mantle. *Geochemistry, Geophysics, and Geosystems* **2**, 2000GC000114.
Kump LR, Kasting JF, Crane RG (2004) *The Earth System*, 2nd edn. Pearson Education, Inc, Upper Saddle River, NJ, p. 419.
Lide D (2000) *CRC Handbook of Chemistry and Physics*, 81st edn. (2000–2001). CRC Press, Boca Raton, FL.
Lindahl PA, Chang B (2001) The evolution of acetyl-CoA synthase. *Origins of Life and Evolution of the Biosphere* **31**, 403–434.
Liss PS, Slater PG (1974) Flux of gases across the air–sea interface. *Nature* **247**, 181–184.
Lynd L, Kerby R, Zeikus J (1982) Carbon monoxide metabolism of the methylotrophic acidogen *Butyribacterium methylotrophicum*. *Journal of Bacteriology* **149**, 255–263.
Madigan MT, Martinko JM, Parker J (2002) *Brock Biology of Microorganisms*. Prentice Hall, Upper Saddle River, NJ.
Margulis L (1982) *Early Life*. Science Books International, Boston, MA.
McCollom T, Seewald J (2003) Experimental constraints on the hydrothermal reactivity of organic acids and acid anions: I. Formic acid and formate. *Geochimica et Cosmochimica Acta* **67**, 3625–3644.
McKay CP, Pollack JB, Courtin R (1991) The greenhouse and antigreenhouse effects on Titan. *Science* **253**, 1118–1121.
Morii H, Koga Y, Nagai S (1987) Energetic analysis of the growth of *Methanobrevibacter arboriphilus* A2 in hydrogen-limited continuous cultures. *Biotechnology and Bioengineering* **29**, 310–315.
Nakamura K, Kato Y (2004) Carbonatization of oceanic crust by the seafloor hydrothermal activity and its significance as a CO_2 sink in the Early Archean. *Geochimica et Cosmochimica Acta* **68**, 4595–4618.
NIST Chemistry WebBook (2003 release), http://webbook.nist.gov/chemistry.
O'Brien JM, Wolkin RH, Moench TT, Morgan JB, Zeikus JG (1983) Association of hydrogen metabolism with unitrophic or mixotrophic growth of *Methanosarcina barkeri* on carbon monoxide. *Journal of Bacteriology* **158**, 373–375.
Ono S, Eigenbrode JL, Pavlov AA, Kharecha P, Rumble DI, Kasting JF, Freeman KH (2003) New insights into Archean sulfur cycle from mass-independent sulfur isotope records. *Earth and Planetary Science Letters* **213**, 15–30.
Pavlov AA, Kasting JF (2002) Mass-independent fractionation of sulfur isotopes in Archean sediments: strong evidence for an anoxic Archean atmosphere. *Astrobiology* **2**, 27–41.
Pavlov AA, Kasting JF, Brown LL, Rages KA, Freedman R (2000) Greenhouse warming by CH_4 in the atmosphere of early Earth. *Journal of Geophysical Research* **105**, 11981–11990.
Pavlov AA, Brown LL, Kasting JF (2001a) UV shielding of NH_3 and O_2 by organic hazes in the Archean atmosphere. *Journal of Geophysical Research* **106**, 23267–23287.
Pavlov AA, Kasting JF, Eigenbrode JL, Freeman KH (2001b) Hydrocarbon aerosols as a source of low-^{13}C kerogens in Archean sediments. *Geology* **29**, 1003–1006.

Pavlov AA, Hurtgen M, Kasting JF, Arthur MA (2003) Methane-rich Proterozoic atmosphere? *Geology* **31**, 87–90.
Prather M, Ehhalt D, Dentener F, Derwent R, Dlugokencky E, Holland E, Isaksen I, Katima J, Kirchhoff V, Matson P, Midgley P, Wang M (2001) Atmospheric chemistry and greenhouse gases. In *Climate Change 2001: the Scientific Basis* (eds Houghton JT, Ding Y, Griggs DJ, Noguer M, van der Linden PJ, Da X, Maskell K, Johnson CA). Contribution of Working Group I to the Third Assessment Report of the Intergovernmental Panel on Climate Change. Cambridge University Press, New York, pp. 239–288.
Prentice IC, Farquhar GD, Fasham MJR, Goulden ML, Heimann M, Jaramillo VJ, Kheshgi HS, Le Quéré C, Scholes RJ, Wallace DWR (2001) The carbon cycle and atmospheric carbon dioxide. In *Climate Change 2001: the Scientific Basis* (eds Houghton JT, Ding Y, Griggs DJ, Noguer M, van der Linden PJ, Da X, Maskell K, Johnson CA). Contribution of Working Group I to the Third Assessment Report of the Intergovernmental Panel on Climate Change. Cambridge University Press, New York, pp. 183–238.
Ragsdale SW (2004) Life with carbon monoxide. *Critical Reviews in Biochemistry and Molecular Biology* **39**, 165–195.
Ratner MI, Walker JCG (1972) Atmospheric ozone and the history of life. *Journal of the Atmospheric Sciences* **29**, 803–808.
Raymond J, Siefert JL, Staples CR, Blankenship RE (2004) The natural history of nitrogen fixation. *Molecular Biology and Evolution* **21**, 541–554.
Riley JP, Chester R (1971) *Introduction to Marine Chemistry*. Academic Press, New York.
Schidlowski M, Hayes JM, Kaplan IR (1983) Isotopic inferences of ancient biochemistries: carbon, sulfur, hydrogen, and nitrogen. In *Earth's Earliest Biosphere: its Origin and Evolution* (ed. Schopf JW). Princeton University Press, Princeton, NJ, pp. 149–186.
Schindler TL, Kasting JF (2000) Synthetic spectra of simulated terrestrial atmospheres containing possible biomarker gases. *Icarus* **145**, 262–271.
Schönheit P, Moll J, Thauer RK (1980) Growth parameters (K_s, μ_{max}, Y_s) of *Methanobacterium thermoautotrophicum*. *Archives of Microbiology* **127**, 59–65.
Selsis F, Despois D, Parisot JP (2002) Signature of life on exoplanets: Can Darwin produce false positive detections? *Astronomy and Astrophysics* **388**, 985–1003.
Sleep NH, Zahnle K (2001) Carbon dioxide cycling and implications for climate on ancient Earth. *Journal of Geophysical Research: Planets* **106**, 1373–1399.
Summons JR, Jahnke LL, Hope JM, Logan GA (1999) 2-Methylhopanoids as biomarkers for cyanobacterial oxygenic photosynthesis. *Nature* **400**, 554–557.
Tian F, Toon OB, Pavlov AA, De Sterck H (2005) A hydrogen-rich early Earth atmosphere. *Science* **308**, 1014–1017.
Tice M, Lowe DR (2004) Photosynthetic microbial mats in the 3416-Myr old ocean. *Nature* **431**, 549–552.
Tyrrell T (1999) The relative influences of nitrogen and phosphorus on oceanic primary production. *Nature* **400**, 525–531.
Van Cappellen P, Ingall ED (1996) Redox stabilization of the atmosphere and oceans by phosphorus-limited marine production. *Science* **271**, 493–496.
Van Trump JE, Miller SL (1973) Carbon monoxide on the primitive Earth. *Earth and Planetary Science Letters* **20**, 145–150.
Walker JCG (1977) *Evolution of the Atmosphere* Macmillan, New York.
Walker JCG, Brimblecombe P (1985) Iron and sulfur in the pre-biologic ocean. *Precambrian Research* **28**, 205–222.
Walter MR (1983) Archean stromatolites: evidence of the Earth's earliest benthos. In *Earth's Earliest Biosphere: its Origin and Evolution* (ed. Schopf JW). Princeton University Press, Princeton, NJ, pp. 187–213.
Walter FM, Berry DC (1991) Pre- and main-sequence evolution of solar activity. In *The Sun in Time* (eds Sonett CP, Giampapa MS, Matthews MS). University of Arizona Press, Tucson, AZ, pp. 633–657.
Watanabe Y, Martini JEJ, Ohmoto H (2000) Geochemical evidence for terrestrial ecosystems 2.6 billion years ago. *Nature* **408**, 574–578.
Westall F (2005) Life on the early Earth: a sedimentary view. *Science* **308**, 366–367.
Woese CR (1987) Bacterial evolution. *Microbiological Reviews* **51**, 221–271.
Xiong J, Fischer WM, Inoue K, Nakahara M, Bauer CE (2000) Molecular evidence for the early evolution of photosynthesis. *Science* **289**, 1724–1730.
Zahnle KJ (1986) Photochemistry of methane and the formation of hydrocyanic acid (HCN) in the Earth's early atmosphere. *Journal of Geophysical Research* **91**, 2819–2834.
Zahnle KJ, Walker JCG (1982) The evolution of solar ultraviolet luminosity. *Reviews in Geophysics and Space Physics* **20**, 280–292.
Zinder SH (1993) Physiological ecology of methanogens. In *Methanogenesis: Ecology, Physiology, Biochemistry, and Genetics* (ed. Ferry JG). Chapman & Hall, New York, pp. 128–206.

APPENDIX 1 THE ATMOSPHERIC HYDROGEN BUDGET

To assess the redox balance in an anoxic atmosphere, one needs to keep track of the atmospheric hydrogen budget (see, e.g. Kasting & Brown, 1998; Kasting & Catling, 2003). Physically, this represents the flow of electrons into and out of the system. In our early Earth atmosphere model, we keep track of four main fluxes in the hydrogen budget:

(1) Volcanic outgassing of H_2 and other reduced species, denoted by $\Phi_{volc}(H_2)$.

(2) H_2 escape to space, denoted by $\Phi_{esc}(H_2)$.

(3) Fluxes of oxidized and reduced chemical species at the lower boundary (defined as positive for upward-flowing reduced species, such as CH_4), denoted by $\Phi_{low}(H_2)$.

(4) Rainout of oxidized and reduced species (defined as positive for downward-flowing reduced species, such as H_2CO), denoted by $\Phi_{rain}(H_2)$.

For convenience, these fluxes are all expressed in terms of H_2. Here, $\Phi_{volc}(H_2)$ and $\Phi_{esc}(H_2)$ represent 'external' fluxes, i.e. fluxes that occur at the boundaries of the overall atmosphere–ocean system. Hence, these terms also appear in Eqn 2 in the main text. In contrast, $\Phi_{low}(H_2)$ and $\Phi_{rain}(H_2)$ represent 'internal' fluxes that describe transfer of hydrogen (or electrons) between the atmosphere and ocean; hence, they do not appear in Eqn 2. Biogenic CH_4 and downward-flowing H_2 are the major contributors to $\Phi_{low}(H_2)$. We express the atmospheric hydrogen balance as:

$$\Phi_{volc}(H_2) + \Phi_{low}(H_2) = \Phi_{esc}(H_2) + \Phi_{rain}(H_2) \qquad \text{(A1.1)}$$

To do a model calculation, we first compute the theoretical value of $\Phi_{esc}(H_2)$ using Eqn 3 and then set $\Phi_{volc}(H_2)$ equal to

$\Phi_{esc}(H_2) + 2\,\Phi_{burial}(C_{org})$, following Eqn 2. In theory, $\Phi_{volc}(H_2)$ represents the volcanic outgassing fluxes of *all* reduced gases, not just H2. However, in practice, we use only the flux of H_2 because the fluxes of the other two main outgassed species, H_2S and CO, are relatively small by comparison. CH_4 is not released by subaerial volcanism (Holland, 1984), although there may be a significant source from submarine volcanism (Kelley *et al.*, 2001, 2005) To compute $\Phi_{low}(H_2)$ and $\Phi_{rain}(H_2)$, we assign each of the 39 long-lived atmospheric constituents an H_2-weighting coefficient as determined by redox stoichiometry. The values of these H_2-weighting coefficients are based on our selection of four 'neutral' atmospheric constituents: N_2, CO_2, H_2O, and SO_2. (We take 'neutral' here to mean neutrality from a redox balance perspective. Our selection of these four particular species is done purely for convenience – we do not need to keep track of the fluxes of 'neutral' constituents.) So, for example, to determine the H_2-weighting coefficients for CO, CH_4, and NO, we first look at the redox reactions that would convert them to their corresponding neutral constituents CO_2 and N_2:

$$CO + H_2O \rightarrow CO_2 + \mathbf{H_2}$$

$$CH_4 + 2\,H_2O \rightarrow CO_2 + \mathbf{4\,H_2}$$

$$NO + H_2 \rightarrow {}^1\!/_2\,N_2 + H_2O$$

From these reactions, we see that 1 mol of CO *produces* 1 mol of H_2, 1 mol of CH_4 *produces* 4 mol of H_2, and 1 mol of NO *consumes* 1 mol of H_2. Thus, the assigned H_2-weighting coefficients for CO, CH_4, and NO are +1, +4, and −1, respectively.

We then multiply the relevant internal fluxes (rainout and lower boundary) for each long-lived constituent by its H_2-weighting coefficient and sum these terms to calculate $\Phi_{low}(H_2)$ and $\Phi_{rain}(H_2)$. This can be expressed mathematically as follows:

$$\Phi_{low}(H_2) = \sum [\Phi_{low}(i) \cdot c(i)] \qquad (A1.2)$$

$$\Phi_{rain}(H_2) = \sum [\Phi_{rain}(i) \cdot c(i)], \qquad (A1.3)$$

where i denotes a long-lived constituent and $c(i)$ denotes its H_2-weighting coefficient.

Evaluating Eqn A1.1 at the end of each model run provides a diagnostic check on the accuracy of the photochemical reaction scheme and on the spatial differencing in the photochemical model. If either of these components does not conserve mass, then the redox budget is not likely to balance. In our models it always balances to better than approximately 0.01%. We note parenthetically that photochemical models that do not keep track of redox balance can produce unphysical results, e.g. high free O_2 concentrations in atmospheres that lack photosynthetic O_2 input (e.g. Canuto *et al.*, 1982; Selsis *et al.*, 2002). Models that do not track redox balance should not be trusted.

APPENDIX 2 CALCULATING DISSOLVED H2 AND CO USING FREE ENERGY CONSTRAINTS

To calculate $[H_2]_{aq}$ in our methanogen-based ecosystems, we apply the free energy form of the Nernst equation to reaction R1. This equation may be written as:

$$\Delta G = \Delta G^0 + R\,T \ln Q, \qquad (A2.1)$$

where
ΔG = free energy change of the reaction,
ΔG^0 = free energy change of the reaction under standard conditions (i.e. unit concentrations of the reactants and products),
R = universal gas constant = 0.008314 kJ mol^{-1} K^{-1}, and
T = 298 K (the assumed water column temperature).

$$Q = \frac{[CH_4]^{\star}_{aq} \cdot a(H_2O)^2}{[CO_2]^{\star}_{aq} \cdot ([H_2]^{\star}_{aq})^4},$$

where $[i]^{\star}_{aq} = \dfrac{[i]_{aq}}{\alpha(i)}$ (that is, the dissolved concentration of species i divided by its Henry's law coefficient; $a(H_2O)$ is assumed to be (1)).

We write Q in this way because the free energies are given in terms of gas partial pressures (in atm), but we are applying Eqn A2.1 to gases dissolved in water. Note that the free energy change between a free gas and a dissolved one is zero when the system is at equilibrium, that is, when the dissolved gas concentration is given by Henry's law. Here, we assume that $\Delta G = -30$ kJ mol^{-1}, i.e. that methanogens will consume dissolved H_2 until they obtain 30 kJ mol^{-1} (the approximate energy needed to produce 1 mol of ATP from ADP + P_i) from R1. Following Kral *et al.* (1998), we assumed that $\Delta G^0 = (-253 + 0.41\,T)$ kJ mol^{-1}; thus, if T = 298 K, then $\Delta G^0 = -131$ kJ mol^{-1}. We take atmospheric CO_2 to be in equilibrium with dissolved CO_2; therefore $[CO_2]^{\star}_{aq} = pCO_2$. To solve for $[H_2]_{aq}$ using Eqn A2.1, we first need to find $[CH_4]_{aq}$. We do this by substituting the photochemical model-calculated value of $\Phi(CH_4)$ into Eqn 1. Thus, we get:

$$[CH_4]_{aq} = \frac{\Phi(CH_4)}{v_p(CH_4) \cdot C} + \alpha(CH_4) \cdot pCH_4 \qquad (A2.2)$$

Solving for Q in Eqn A2.1 gives $Q = \exp\left(\dfrac{\Delta G - \Delta G^0}{RT}\right)$. We then solve for $[H_2]_{aq}$ using the definition of Q and the value of $[CH_4]_{aq}$ obtained from Eqn A2.2:

$$[H_2]_{aq} = \alpha(H_2) \cdot \left[\frac{[CH_4]^{\star}_{aq}}{pCO_2} \cdot \exp\left(\frac{\Delta G^0 - \Delta G}{RT}\right)\right]^{\frac{1}{4}}. \qquad (A2.3)$$

Using a similar approach, we calculate $[CO]_{aq}$ for Cases 2 and 3. For these calculations, we apply Eqn A2.1 to R6. We assume that the primary acetogens would consume CO until

they obtain 30 kJ mol^{-1} from R3, and that the acetotrophic methanogens would consume the resulting CH_3COOH until they obtain 30 kJ mol^{-1} from R5. Thus, using Hess's law, we assume that the combined action of these two groups of organisms would yield 60 kJ mol^{-1} from R6.

Here, $Q = \dfrac{([CO_2]^{*}_{aq})^3 \cdot [CH_4]^{*}_{aq}}{([CO]^{*}_{aq})^4 \ (a(H_2O))^2}$. Applying the Gibbs equation ($\Delta G^0 = \Delta H^0 - T \cdot \Delta S^0$) to R6 gives us $\Delta G^0 = -241.5 + 0.104 \cdot T = -210.5$ kJ mol^{-1} for T = 298 K. We again take atmospheric CO_2 to be in equilibrium with dissolved CO_2, and we calculate $[CH_4]_{aq}$ using Eqn A2.2. Finally, we solve for $[CO]_{aq}$ just as we did above for $[H_2]_{aq}$:

$$[CO]_{aq} = \alpha(CO) \cdot \left[(pCO_2)^3 \cdot [CH_4]^{*}_{aq} \cdot \exp\left(\frac{\Delta G^0 - \Delta G}{RT} \right) \right]^{\frac{1}{4}}$$

APPENDIX 3 ABIOTIC UPTAKE OF ATMOSPHERIC CO BY THE OCEAN

For a biosphere in which there were no CO-consuming organisms (e.g. our Case 1), atmospheric CO should still have flowed into the ocean, but at a relatively slow rate that was controlled by abiotic chemistry. This process has been studied in the laboratory by Van Trump & Miller (1973) and more recently by M. Schoonen and R. Penfield at SUNY Stony Brook (private communication). After it enters the ocean, CO hydrates to produce formate ($HCOO^-$). This process involves three steps: (1) dissolution of atmospheric CO to form dissolved CO, (2) hydration of CO to formic acid, HCOOH, and (3) dissociation of HCOOH to $HCOO^-$ and H^+. Hydration of CO to formic acid is the rate-limiting step. The overall reaction can be represented as follows:

$$CO + OH^- \rightarrow HCOO^- \qquad \text{(RA3.1)}$$

Schoonen and Penfield have examined the photochemical as well as thermal decomposition of this resulting $HCOO^-$. They found that a small fraction of it (approximately 4%) is photochemically converted into acetate, CH_3COO^-. This represents a net loss of CO from the system. However, most of it gets converted back into CO, either by photochemical processes in the surface ocean or by thermal processes in the deep ocean.

We have created a 2-box model that allows us to estimate the abiotic deposition rate of CO (Fig. A3.1). Our model includes four variables:

(1) dissolved CO in the surface ocean, $[CO]_s$;
(2) dissolved formate in the surface ocean, $[HCOO^-]_s$;
(3) dissolved CO in the deep ocean, $[CO]_d$;
(4) dissolved formate in the deep ocean, $[HCOO^-]_d$; and

At steady-state, production equals loss for each of these chemical species. We can express this by the following system of equations (production terms are on the left-hand side of each equation, loss terms are on the right):

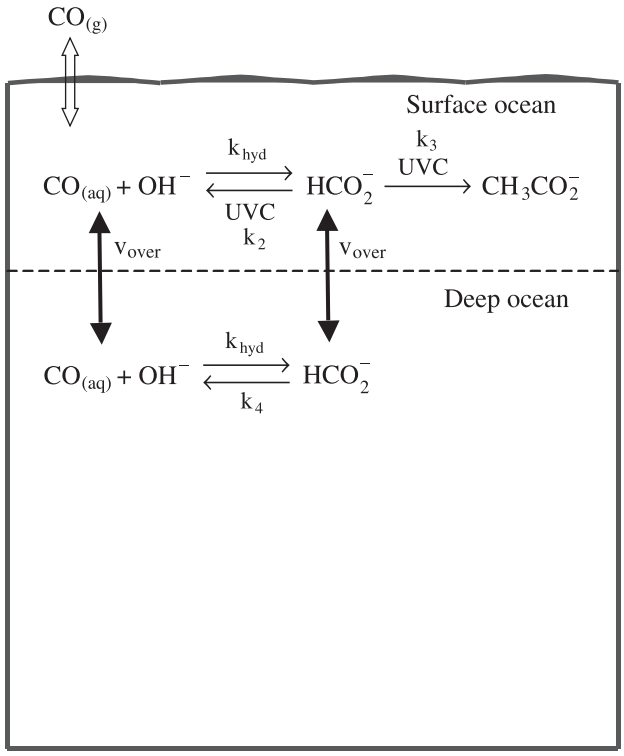

Fig. A3.1 Diagram of 2-box model of CO deposition for a biosphere in which there are no CO-consuming organisms. Terms are explained in the text.

$[CO]_s$:

$$v_p(CO) \cdot (\alpha_{CO} \cdot pCO - [CO]_s) \cdot C + k_2 \cdot [HCOO^-]_s \cdot z_s \cdot C = k_{hyd} \cdot [OH^-]_s \cdot [CO]_s \cdot z_s \cdot C + v_{over} \cdot ([CO]_s - [CO]_d) \cdot C \qquad \text{(A3.1)}$$

$[HCOO^-]_s$:

$$k_{hyd} \cdot [OH^-]_s \cdot [CO]_s \cdot z_s \cdot C = k_2 \cdot [HCOO^-]_s \cdot z_s \cdot C + k_3 \cdot [HCOO^-]_s \cdot z_s \cdot C + v_{over} \cdot ([HCOO^-]_s - [HCOO^-]_d) \cdot C \qquad \text{(A3.2)}$$

$[CO]_d$:

$$v_{over} \cdot ([CO]_s - [CO]_d) \cdot C + k_4 \cdot [HCOO^-]_d \cdot z_d \cdot C = k_{hyd} \cdot [OH^-]_d \cdot [CO]_d \cdot z_d \cdot C \qquad \text{(A3.3)}$$

$[HCOO^-]_d$:

$$k_{hyd} \cdot [OH^-]_d \cdot [CO]_d \cdot z_d \cdot C + v_{over} \cdot ([HCOO^-]_s - [HCOO^-]_d) \cdot C = k_4 \cdot [HCOO^-]_d \cdot z_d \cdot C \qquad \text{(A3.4)}$$

Here,
z_s = depth of surface ocean = 10^4 cm
z_d = depth of deep ocean = 3.9×10^5 cm
v_p(CO) = piston velocity of CO = 5×10^{-3} cm s^{-1}
v_{over} = turnover velocity of ocean = 1.2×10^{-5} cm s^{-1}
$[OH^-]$ = concentration of OH^- (for pH = 8, $[OH^-] = 10^{-6}$ mol L^{-1})

α_{CO} = Henry's law coefficient for CO = 8×10^{-4} mol L^{-1} bar^{-1}
pCO = partial pressure of CO (taken from photochemical model output)
$C = 6.02 \times 10^{20}$ molecules cm^{-3} mol^{-1} L^{-1} (units conversion factor)
k_{hyd} = rate coefficient for CO hydration to $HCOO^-$ = exp(−10,570/T + 25.6)
k_2 = rate coefficient for photochemical conversion of $HCOO^-$ to CO ≈ 6.4×10^{-5} s^{-1}
k_3 = rate coefficient for CH_3COO^- formation from $HCOO^-$ ≈ 2.7×10^{-6} s^{-1}
k_4 = rate coefficient for thermal conversion of $HCOO^-$ to CO ≈ 8.04×10^{-14} s^{-1}

Except for k_4, the values for the rate coefficients were provided by M. Schoonen and R. Penfield; the value for k_4 was extrapolated from McCollom & Seewald (2003). Note that we have applied the stagnant boundary layer to the exchange of CO between the atmosphere and ocean, as reflected in Eqn A3.1. Also, we have simplified the system by assuming no pH gradient in the ocean, so that $[OH^-]$ does not vary with depth. This should be approximately true for an abiotic ocean because the pH gradient is set up by the downward flux of organic matter from the surface to the deep ocean. Finally, it is also worth noting that because of the very large difference between the photochemical and thermal decay coefficients for formate (k_2 and k_4, respectively), it would be reasonable to infer that formate could have accumulated to much higher levels in the deep ocean than it did in the surface ocean. This could have had important implications for the prebiotic chemistry of the ocean.

Using values of pCO obtained from the photochemical model, we solve the above system of 4 equations and 4 unknowns. We then use the model-calculated value for $[CO]_s$ to find the CO deposition velocity, v_{dep}(CO), based on Eqn 1:

$$v_{dep}(\mathrm{CO}) = \frac{v_p(\mathrm{CO}) \cdot (\alpha_{CO} \cdot p\mathrm{CO} - [\mathrm{CO}]_s) \cdot C}{n_{CO}}, \quad \text{(A3.5)}$$

where n_{CO} = number density of CO.

Using this approach, we have found that for a wide range of plausible ocean temperatures, the CO deposition velocity should be of the order of 10^{-8}–10^{-9} cm s^{-1} in the abiotic case. These values may be compared with CO deposition velocities of approximately 10^{-4} cm s^{-1} for the case when dissolved CO is consumed by organisms (see Model Description section). A sensitivity test reveals that the surface ocean temperature would have to be unrealistically high (over 200 °C) for the abiotic CO deposition velocity to approach the biotic value. When the low, abiotic CO deposition velocities are used in the photochemical model, we find that CO runaway occurs for high CH_4 and/or CO_2 values. As explained in the text, CO runaway may actually have occurred if methanogens evolved before CO-consuming organisms did. There is, however, no geological evidence that such an unusual atmospheric state ever existed.